UNIVERSITY OF CALIFORNIA

Santa Barbara

Detection of biomarkers using DNA biosensors in a fluorescent platform to improve current one-step point-of-care methodologies

A thesis submitted in partial satisfaction of the

requirements for the degree Master of Science

in Chemistry

by

Hannah Marie Kallewaard-Lum

Committee in charge:

Professor Kevin Plaxco, Chair

Professor Stanley M. Parsons

Professor R. Daniel Little

Professor Deborah K. Fygenson

June 2016

The thesis of Hannah Marie Kallewaard-Lum is approved.

_____
R. Daniel Little

_____
Deborah K. Fygenson

_____
Stanley M. Parsons

_____
Kevin Plaxco, Committee Chair

June 2016

Detection of biomarkers using DNA biosensors in a fluorescent platform to improve current one-step point-of-care methodologies

by

Hannah Marie Kallewaard-Lum

ACKNOWLEDGEMENTS

As I like to point out, science is never conducted in a social vacuum, though sometimes in an actual vacuum. Without the continuous moral support from my best friend for life Dave I would have left the program sooner with little to say for my time spent learning many techniques and skills. Thank you for all the support you gave me during my program, especially toward the end.

All the Biochemistry sub-students on the first floor helped me out in various ways. My cohort, Adam, Elicia, Faye, Paul, Andrew, and Ben had my back when we were starting out taking lots of classes together. Dean, Kota, and Clay taught me many techniques on the actual biochemistry side of things.

The core group of ladies that helped me re-learn all the chemistry information to study for the entrance exams. Sara and Meredith also gave continuous perspective on life in the sun for our lunches at noon. The continuous support from these women also helped me get through the dark and lonely times of research.

Those in my lab that helped me figure out which way was up, and creating exit strategies when I could no longer think: Netz, Hui, Martin, and Phillipe. To Jacob for the unwavering support all the years. To the young-ins Megan and Shruti who always were ready for drinking wine or running ten miles, just keep focus on getting out and how to most efficiently achieve that goal.

I'd also like to thank my dog Threo, even though he can't read this. Your antics of playing with your squeaky squirrel and the many other toys always brightened my day. If

not, a cute sweater and hiking boots always made me smile. On the days that weren't great, you were a great tissue, and always let me cuddle you until I could find the silver lining.

Finally I'd like to thank my entire committee, who supported my inquisitive nature, mentored me through your actions, and provided wonderful guidance all these years

ABSTRACT

Detection of biomarkers using DNA biosensors in a fluorescent platform to improve current one-step point-of-care methodologies

by

Hannah Marie Kallewaard-Lum

Current methodologies for patient diagnosis require the use of skilled workers, expensive reagents, instrumentation, and most importantly, time. As these methodologies encourage inconsequential follow-up between patients and their doctors, new methods must be developed. These methods should follow the World Health Organization (WHO) ASSURED guidelines (Accessible to those in need, Sensitive to the clinical range of the target of interest, Specific to the target of interest with no false positives or negatives, User-friendly, Rapid, under one hour for results, Equipment free, and Delivered to those in need) to create point of care technologies available for all. To this end, my studies focus on the development of convenient calibration methods for use with fluorescent, aptamer-based biosensors (aptamer beacons). Specifically, I describe here the creation, characterization, and application of a one-tube method for the calibration of aptamer beacons using sensors for the detection of DNA, silver ions, and thrombin as my test bed.

A significant hurdle in the point of care testing of biomarkers in complex solutions is that there is sample variation, requiring large volumes of the target of interest and complex and cumbersome calibration. In response, I have created a simple, three-step, one-tube method for the calibration of aptamer beacons supporting the direct quantification of

specific target molecules within complex sample matrices. Specifically, I have shown that the sequential addition of two inexpensive and stable oligonucleotide-based reagents allows for the determination of the absolute minimum and maximum fluorescence produced by the sensor in each solution, providing the information to calibrate in the face of sample-to-sample variations in a simple, single-tube format. Using these three measurements together with the pre-determined disassociation constant of the aptamer, I demonstrate the single-tube calibrated quantification of multiple targets directly in complex samples.

TABLE OF CONTENTS

LIST OF FIGURES

Chapter 1. Introduction

1.1 Molecular Diagnostics

The molecular markers associated with infectious diseases,[1,2] oncology,[3] pharmacogenomics,[4] genetic disease screening,[5] antigen typing,[6] and blood biomarkers[7,8] spurred the world of molecular diagnostics. This type of testing determines any changes from a normal sequence in a specific space of deoxyribonucleic acid (DNA) or ribonucleic acid (RNA) sequences,[9] the concentration of some protein or small molecule biomarker, and the detection and quantification of specific pathogens.[10]

Current molecular diagnostic testing technology requires multiple steps and transfers, but most importantly, it often takes days until the patient is diagnosed.[11] Only after a patient enters the doctor's office can the doctor decide to order a blood test since patients cannot order their own testing. The patient then must travel to a phlebotomist, sometimes in the same facility or possibly in another location. Once there, the process of drawing the patient's blood is performed, which can be difficult for a person who is dehydrated, cold, undernourished, or simply has small veins. Upon collection, the blood sample, it is then labeled and transported to the central laboratory for testing.

Central laboratories are specialized facilities that receive samples from local collection centers and perform a range of complex testing protocols. This testing requires skilled workers who have been educated in techniques and troubleshooting of expensive and specific equipment and reagents. A knowledgeable staff runs the equipment and interprets results. This "overhead" costs large sums of money, which is why modern molecular testing uses the central laboratory framework rather than using smaller testing sites located close to or at the point of care e.g. hospital, doctors offices, operating areas, etc.

An additional factor for the centralized facilities approach to molecular diagnostics is the complexity of current testing approaches. Once a sample arrives at the central laboratory, it queues for the many steps it must undergo to complete testing. Frequently samples are batch tested;[12] meaning many samples destined for the same type of testing must be collected before the test is run. Although this saves the company money, it costs the patient precious time in obtaining a diagnosis. In addition, whole blood samples often cannot be used directly for the testing, but instead must be centrifuged to separate the sample into serum and red blood cells. Some tests require even more processing of the blood sample. Every test is then run in triplicate to validate results, and calibrations are verified for proper reporting. The results are then sent back to the doctor for reporting. The entire process takes anywhere between a few days to six months, painfully slow for patients whose health management depends on the results.

The centralized facility approach to testing significantly harms healthcare for patients. This method cannot be completed within the average doctor visit of 10 minutes, thus requiring a follow-up visit between the doctor and patient. However, research shows deficient patient follow up if a second contact is required, especially in low-resource areas. [13] Usually, it is crucial for the patient to receive counseling on the results and to determine the path of treatment.

To combat these lengthy testing times and expensive testing, there is a push toward point-of-care technologies. The term point-of-care simply means that the test can be easily administered wherever the test is needed and gives results in a reasonable amount of time. The World Health Organization (WHO) has set guidelines for this type of testing with a mnemonic acronym, ASSURED.[14] These guidelines dictate that tests should be:

Accessible to those in need

Sensitive to the clinical range of the target of interest

Specific to the target of interest, no false positives or negatives

User-friendly

Rapid, under one hour for results

Equipment free

Delivered to those in need

Testing that remains within these guidelines solves many of the problems outlined above in regard to lengthy and expensive testing. Thus, these technologies can significantly improve outcomes and costs for patients by shortening time to diagnosis, and therefore treatment.

Although some progress toward WHO-approved point of care devices has been achieved, much remains to be achieved to reach these goals fully. Excellent examples of current point-of-care testing are seen in urine dipsticks, glucose meters, and urine pregnancy tests. Most of these tests separate the target protein or analyte from a complex solution, amplify the target, and then detect the target all in one system. The urine pregnancy test is an example of a lateral flow test, where the target human chorionic gonadotropin (hCG)[15] is separated from the urine in the initial absorbent material, and then the hCG is concentrated by binding to an antibody which is covalently bound to an optical reporter. Then this complex binds to another antibody for hCG in a pattern that can be read by the user. Distinctly, testing like the pregnancy and urine dipsticks are qualitative, providing only yes or no answers. While this works well for pregnancy, other types of testing require quantitative results to understand outcomes, such as the glucose measurements diabetics use to determine their need for insulin. Unfortunately, the technology behind glucose monitoring

cannot be applied to other targets. This is because the specific enzyme that detects glucose converts it into hydrogen peroxide, which is read electrochemically.[16] Very few recognition enzymes are able to turn their targets into electrochemically active products for detection. Instead, progress requires technologies with a new approach that remains within the WHO guidelines.

To better understand new approaches to point of care technologies, it is important to understand the gold standards used for current testing methods. These techniques involving microarrays, the polymerase chain reaction (PCR), and Enzyme-Linked Immunosorbent Assays (ELISA), are often modified from their existing platforms in an effort to create point of care methodologies. Scientists pushing technologies forward often pull from these established methods habitually, as they are well understood by the scientific community.

1.1.1 Microarrays

This type of testing, also called multiplexing, is used to simultaneously screen a wide range of binding events, allowing for large sets of data to be collected.[17] As compared to other arrays, microarrays use small volumes in small spaces. Inspired by ELISAs that used 196+ well plates, microarrays have been used to miniaturize the detection process, demanding less material while maintaining high specificity and selectivity. Since the first publication on microarrays, where the grid was a 1x1 cm grid with 400 individual spots, the grids have somewhat expanded in size while the number of spots has increased significantly.[18]

Binding events can be DNA or RNA binding for the determination of a mutation such as a single nucleotide polymorphism (SNP). This approach also allows for multi-drug

screening, in which many drugs of interest are screened against a targeted protein. In the same vein, protein-protein binding can also be evaluated such as antigen typing and epitope (antigen recognition domain) and surface protein determination can also be evaluated. In general, the binding event produces an optical signal, typically a change in intensity, which is then read to determine the level of binding.

Generally, this technique involves three or more steps and at least a half a day to run one experiment from sample prep to signal output. The central technology is a 2D array on a surface such as glass or thin-film silicon, where the capture molecule is bound to the surface. A sample of interest is then applied to the array. If the purpose of the experiment is sequencing DNA or RNA, the nucleotides must first be extracted from the source, which typically requires the lysing of cells followed by centrifugation for the elimination of any other molecules. If instead, a whole cell is used, e.g. for surface protein detection, no such preparation is required. In either case, after application of the sample to the array, an incubation period is required to ensure binding. Then a wash step is performed to remove any non-binding material. The final requirement is the introduction of some sort of optical reporter to determine the level of binding, which requires additional application and wash steps before detection. A fluorescently labeled antibody can be used in protein and certain small molecule detection assays. DNA and RNA probes are often labeled with dyes before being added to the array. Finally, detection of the optical reporters is performed to determine which spots indicate binding events. This information is used to deduce which mutations, proteins, or types of cells were present in the sample.

There are many examples of the use of microarrays in point-of-care technology because they provide the sensitivity and selectivity required from testing with a multiplexed

approach. This includes testing such as a lateral flow allergen microarray[19], protein microarray for neonatal sepsis diagnosis[20], and detection of mutations in *KRAS* and *p53* genes[21]. These assays detect specific antibodies, non-antibody proteins, protein-protein interactions, cell surfaces, and DNA or RNA sequences all while using small volumes of reagents. Nonetheless, these assays are complex and time-consuming, requiring multiple reagents, washing steps, require the use of expensive readers, and specialty spotting instruments. Although the scientific community is combating expensive readers by coding programs for cell phone cameras, there has been no improvement speeding up the required steps to get to optical detection.

1.1.2 Polymerase chain reaction (PCR)

Polymerase chain reaction, or PCR, is currently the gold standard for detection of DNA or RNA strands and fragments. This method relies on specific instrumentation, reagents, and energy to heat and cool the system for the replication of DNA or RNA to occur. The technique involves five steps, with a half day often required just to perform the amplification. Depending on the detection method employed, an additional half-day or more is often needed before detection can be reported. The first step in PCR is designing primers, short DNA sequences that attach upstream of the sequence of interest and allow the DNA or RNA polymerase protein complex to bind and begin replication. Once the proper primers, Taq polymerase (from *Thermus aquaticus*), nucleotides, and buffer are added, the reaction solution, it is heated to 95 °C to denaturation the double stranded oligonucleotides. The solution is then cooled to just below 70 °C to allow primers to anneal to the target strands. The solution is then heated slightly to 72 °C, enabling the extension of the primers by the

polymerase, which creates copies of the target. These heating and cooling steps make up one cycle, which is repeated around 30 times to amplify enough of the target for detection. The final step is the detection of the amplified oligonucleotide. This can be a simple gel electrophoresis if only based on molecular weight; however in the case of disease determination, each base requires sequencing for the accurate diagnosis.

There are many variations on the method described above for increased specificity, and target validation; however, none have achieved applicability for point-of-care. One method, helicase-dependent PCR, eliminates the need for thermocycling but requires a second protein, increasing the price of the method and requiring optimized buffers and primers to produce reliable results.

Some adjustments have been devised to make the required instrumentation suitable for point-of-care. A major focus has been on creating smaller and less expensive versions of the thermocycler, undoubtedly a crucial instrument in this method. With low-income areas in mind, Walker and coworkers were able to create a thermocycler from a computer.[22] Even so, the PCR method still requires expensive reagents, time, and skilled workers.

1.1.3 Enzyme-linked immunosorbent assay (ELISA)

The enzyme-linked immunosorbent assay, or ELISA, is the current gold standard for the detection of protein biomarkers.[23] This technique is ideal for research or clinical situations where skilled workers perform the testing in controlled environments with all reagents readily available. Since workers perform these experiments for the detection of proteins, which are often present in low concentrations, this technique requires the use of long incubation times and many wash steps to ensure specificity.

Generally, the ELISA technique requires a minimum of three steps, each with an incubation time between 2 and 16 hours. It is typically performed in 94-well plates where a control can be performed at the same time as the samples. In the first step, the target is exposed to the surface and allowed to adhere, often through non-covalent binding. Sometimes an additional step to pre-modify the surface for the target attachment is required. For example, in sandwich ELISAs, an antibody specific to the target is adhered to the surface before the sample with the target is presented. Once the target has bound to the surface of the plate, a wash step is performed to remove excess solution, and remove other proteins, not of interest. In the second step, another target-specific antibody is added to sandwich the target. A second wash step is performed to again remove any antibody not bound to the target. The final step is the reporting method. This can be a fluorescently modified antibody used in step 2, or a secondary antibody that recognizes and binds the first antibody, and is covalently modified with a fluorescent reporter or the enzyme horseradish peroxidase (HRP). In the latter case the enzyme converts hydrogen peroxide into a colored solution and the enzymatic reaction is stopped with sulfuric acid.

A well-developed ELISA method is specific and sensitive but severely user-unfriendly because it is time-consuming and requires many reagents. In addition, while ELISA ultimately works well, each new target requires significant development of buffers, washes, incubation times, and antibodies to achieve consistent and reliable results.

1.2 The Rise of Aptamers

While the methods involving ELISA, PCR, and microarrays demonstrate their abilities of detecting small quantities of a target with high specificity, they all also require

time-consuming steps with multiple specialized reagents, wash steps, and complex, expensive equipment. This section describes how aptamers offer a potentially valuable step forward in molecular diagnostics, providing a means for reducing the time needed for time to detection, the number of reagents required and the overall cost, while maintaining specificity and sensitivity.

1.2.1 Aptamer Background

Aptamers are single stranded nucleotide sequences that bind a variety of targets from small molecules to large proteins with high specificity and selectivity. Advantageously, these sequences are small, thermally stable, and inexpensive to synthesize. Aptamers also outperform other systems in single-step sensing platforms by undergoing large-scale conformational changes that generate a specific output signal. By contrast, however, aptamers with high specificity against a target can be difficult to experimentally create and their functionality in often condition-dependent.

Aptamer are identified, rather than rationally designed using the Systematic Evolution of Ligands by Exponential Enrichment (SELEX) method pioneered by Tuerk and Gold.[24] In the first step of SELEX, a large DNA or RNA library of 10^{15} or more individual sequences, are incubated with the target molecule. Sequences are then separated by washing away non-binding sequences. Compatible, bound, sequences are eluted under more stringent conditions, amplified, sequenced, and prepared for a subsequent round of selection. In addition to multiple rounds of positive selection, a negative selection based on a derivative of the target is used to increase specificity by eliminating any sequences that bind to the

derivative. To create an aptamer, five or more rounds of selection with at least two rounds of negative selection are used.

1.2.2 The First Aptamers

Originally aptamers were created for affinity chromatography to bind both organic dye molecules and nucleic acid binding proteins.[25] Compared to the standard methods used at the time, aptamers were less expensive while still maintaining the specificity required for affinity chromatography. These original aptamers were made with RNA bases, and DNA aptamers did not arrive until a few years later.[26,48] Aptamers were a major improvement to methods like ELISA and PCR due to their stability at room temperature and fast binding kinetics.[27]

DNA aptamers against alpha-thrombin,[31] cocaine,[28] platelet-derived growth factor (PDGF), immunoglobin E, and adenosine triphosphate (ATP) dominate the literature landscape.[29,30] These aptamers are among the original aptamers and are robust systems used repeatedly across the scientific community.[31] Research groups often use one of these aptamers as a model system for proving new technologies and methodologies.

With increasing numbers of scientists working in the aptamer field, single targets started seeing multiple aptamers. For example, alpha-thrombin currently has two unique aptamers. The first, a fifteen-base aptamer, creates a g-quadruplex upon binding with the protein at an allosteric site.[32] A g-quadruplex is a structure in both DNA and RNA where four guanine bases associate through Hoogsteen hydrogen bonding to form a square planar shape. This structure can be created from one strand, or many strands where the backbone can be either parallel or anti-parallel.[33] Two or more g-quadruplex structures can stack on

top of each other as seen in the 15-base alpha-thrombin aptamer, which has a stack of two.[34] A second, twenty-seven-base aptamer against thrombin includes both the g-quadruplex structure and a stem and binds a different allosteric site on thrombin, such that it resembles a candy cane shape; the g-quadruplex being the hook and the stem wrapping itself down the long part of the candy cane.[35] Some researchers have used both alpha-thrombin aptamers to identify the protein at lower concentrations allowing for better detection.[36,37] Another advantage of using two aptamers is the allowance for a sandwich-like assay in which the first aptamer can be attached to a surface for capturing the protein, and the second aptamer can be used for detection with an optical reporter. This constitutes an extension of the ELISA method with antibodies replaced by aptamers.[38] Since aptamers require shorter binding incubation times than antibodies, their use speeds up the time to diagnosis.

1.2.3 Aptamers in Diagnostics

As noted above, the first aptamers were made from RNA. This was due to the recent discovery of their active participation in cell signaling, not just carrying genetic information.[39] Many of the attempts at converting RNA aptamers to DNA sequences resulted in decreased affinities, even when the structures were nearly identical.[40,41] Although it is rare that an aptamer directly converted from RNA to DNA performs identically, the dopamine aptamer held all of its properties.[42] Also, as noted previously, aptamer affinities are notoriously dependent on the conditions of the experiment, which include the backbone of the aptamer for binding the target of interest.[43]

The use of aptamers in diagnostics proves difficult when using real samples of serum or whole blood, or working directly in *in vivo*. Proteins within these solutions rapidly break

down the oligonucleotides by hydrolyzing the bases, thereby eliminating the aptamer and its ability to detect the target of interest. Various modifications are made to aptamers to prolong their life in diagnostic samples, however that is not the focus here.[43]

With the discovery of aptamers, efforts to harness them for diagnostic purposes bloomed. One example is a qualitative lateral flow test for cocaine.[44] In this test, streptavidin-coated gold nanoparticles (AuNP) are additionally coated in the cocaine aptamer, and allowed to aggregate. The aggregation of AuNPs produces a distinct red color. In the presence of cocaine, the aptamer folds around its target and disassociates from the AuNPs. The dis-aggregated AuNPs then flow through a filter binding to a biotin strip, creating a red line. This test is able to function in complex solutions such as saliva, urine, and blood serum due to the filtering nature of the lateral flow strip. Another example uses both AuNPs and quantum dots (QD) to detect both cocaine and adenosine independently in the same sample.[45] Here, the aptamer is conjugated to the QD, and a hybridizing strand is conjugated to AuNPs. When the solutions are mixed, a low luminescence is observed as a result of the hybridization of the aptamer with its hybridizing strand, bringing the QDs and AuNPs in close proximity to one another. Upon addition of the target, the aptamer folds and releases the hybridizing strand, thereby separating the complex and resulting in high luminescence. By conjugating the cocaine aptamer and the adenosine aptamer on QDs with different wavelengths, one solution can independently determine either target. This system performed well in 10 % serum but required overnight incubation for best results.

Another use of diagnostic aptamers is the labeling of malignant cells. The protein mucin (MUC1) is a glycoprotein found on epithelial cells. While present on healthy cells, it is expressed in 10x higher concentrations on extracellular membranes of in cancerous cells.

The use of aptamers rather than antibodies for labeling *in vivo* allows for a much faster clearance of unbound probes. Non-binding antibodies take a time to clear from the cells, extending the time required for accurate detection. The aptamer against MUC1 can be modified to include a mercaptoacetyl diglycine (MAG_2) ligand which complexes with technetium.[46] When this aptamer complex is loaded with radiolabeled ^{99}Tc, it can be injected into mice where the aptamer will detect the MUC1 glycoprotein. To determine the organs where MUC1 has mutated, the detection of gamma-rays is performed in a scintillation counter.[47]

1.3 Structure-Switching Aptamers

As their name suggests, structure-switching aptamers are dynamic and transition between two different structures. One structure does not bind the target while the other does. As such, target binding causes a conformational change. The first example of the use of structure-switching aptamers comes ten years after the appearance of aptamers in literature.[25,73] An advantage of this type of aptamer is that it allows for direct detection of target when using an output such as fluorescence. Thus, the binding of the target of interest creates a signal from the aptamer that reports on the concentration of the target in a solution.

The first use of a structure-switching aptamer was reported in 2001 when Hamaguchi and co-authors described the use of the 15-base thrombin aptamer as a starting point.[48,73] They modified the aptamer by adding 4 to 6 added bases to produce a stem-loop structure in the absence of thrombin. These added bases bind the middle of the g-quadruplex, disrupting both the quadruplex structure and protein binding. With this new aptamer, the researchers

were able to detect thrombin at an apparent disassociation constant of 10 nM, a vast improvement over the original 200 nM.

Since 2001, the use of structure-switching aptamers has increased. Luminescence the detection of immunoglobulin E (IgE),[49] and fluorescence detection of platelet-derived growth factor (PDGF),[50] cocaine,[51] and adenosine triphosphate (ATP)[52] have all been achieved using structure-switching aptamers.

During SELEX, aptamers can be designed to unbind a sequence upon target binding. In this system a small sequence, between 7 and 15 bases is added for hybridizing another DNA strand. This sequence is placed in the middle of the DNA library so that upon binding to the target the hybridization is disrupted. To create a signal-on structure-switching aptamer, a quencher is added to the hybridizing strand. The quencher stays in close proximity to the fluorophore when hybridized. Then when the aptamer binds the target, the quenching strand is displaced, allowing for increasing fluorescence. Nutiu and Li detail this system in the creation of an ATP structure-switching aptamer after performing 16 rounds of selection.[53]

1.3.1 Designing Structure-Switching Aptamers

In the absence of explicit selection for structure switching, not all aptamers switch between non-binding and binding conformations. To create a direct-detection, structure-switching aptamer modification from a parent sequence is preferred. This design effort can prove easier if it is known how the aptamer binds its target, but a number of methods demonstrate proficiency even in the absence of this information.

Naturally, understanding the target-binding region of an aptamer sequence provides insight into the system. Aptamers are raised with primer tails on either side of a sequence to enable amplification. These primer sequences can inadvertently be involved with target binding. Most selections performed today take precautions to ensure primers are not involved with binding. Truncation studies aid in determining the sequence required for binding. Although any change in sequence could result in a decrease in binding affinity between the aptamer and the target, performing truncation studies in a logical manner helps maintaining the best binding affinity. Regardless, aptamers are often reported with primers and with only limited truncation studies.

Ideally, a co-crystallization or nuclear magnetic resonance (NMR) resolved structure of the aptamer and its target will accurately determine the binding location. While this is easier with small molecules, as they are small and more static, there are instances of well-established aptamers that have no crystal structure. Generally, enzymes are difficult to crystallize without a cofactor to hold the enzyme in a static state, and as such, there are only a few enzyme-binding aptamers co-crystalized with their target.[54] Additional challenges in crystallizing the target with the aptamer arise are due to the flexibility of aptamers the unbound state.

1.3.2 Additional Oligonucleotides for Detection

In a second approach to inducing aptamers to switch between two structures, additional oligonucleotide strands were added and designed into the system.[55] As mentioned previously the fluorophore and quencher are on separate strands rather than contained in the same strand. Upon target binding, the second strand is displaced, separating the fluorophore

and quencher, thus producing fluorescence. Another option is to split the aptamer into two different strands that only come together upon binding of the target. In this system, a decrease in fluorescence is seen when using a fluorophore and quencher, or a change in fluorescence emission wavelength is seen with overlapping fluorophores.

Alternatively, a quenching strand added to the aptamer for hybridization can also cause structure switching. Chen et. al. used this method with their aptamer for ochratoxin A, a food-born toxin.[56] The 36-base fluorescein-labeled aptamer was hybridized to a quencher-labeled strand of nine to thirteen bases. In addition, the authors looked at the ratio of the aptamer to quencher strand to optimize the system. In the end, they used the 10-base quenching strand with a 1:3 ratio of the aptamer: quenching strand in real corn samples.

The addition of these extra oligonucleotides vastly improved the variety of aptamers able to directly detect the binding of the target. However, such additional oligonucleotides only add to the number of reagents required to produce results. As WHO guidelines recommend point-of-care testing be as user-friendly as possible, additional reagents for the simple detection of a target is sub-optimal. This type of aptamer system was included here however as a stepping-stone to systems with internal controls, as explained in the next section.

1.3.3 Internal Controls for One-tube Detection

As per the WHO strategy for point-of-care testing, rapid testing helps ensure that a patient obtains the advice and treatment indicated by the test. To make testing rapid, the use of complex solutions is required. As aptamers are susceptible to degradation in these

complex solutions, the employment of an internal control is needed to ensure accurate detection of the target.

One example of the use of an internal control comes from the Yingfu Li group in the detection of theophylline in human serum samples.[57] The system requires the use of four strands as follows. The first strand is the aptamer, with additional bases for binding the other strands. The second strand hybridizes to the aptamer section of the first strand at the 3' end and contains a quencher at its own 3' end. The third strand sits in the middle of the first strand and presents two different fluorophores on each end. Finally, the fourth strand hybridizes to the 5' end of the first strand with a quencher on its own 5' end. This set up allows the first fluorophore to fluoresce upon the binding of the target. However, a false positive occurs if the second fluorophore signals indicating endonuclease activity through the cleavage of the strands. While this internal control provides identification of endonuclease activity on the aptamer, there could still be changes in fluorescence from sample to sample with no way to accurately compare the target concentrations between samples.

Our group pushed these established boundaries to include internal controls that could account for sample variation. Vallée-Bélisle et al. used a DNA sequence to detect transcription factors, proteins that recognize double-stranded DNA to initiate the transcription of DNA into messenger RNA (mRNA).[68] In addition to this transcription factor aptamer, a competitor and stabilizer strand were used. The competitor strand binds the target transcription factor, removing the target from the aptamer. This returns the aptamer to the baseline fluorescence. The stabilizer strand binds the aptamer in the target binding form, such that maximum fluorescence is achieved with no added target. With these three

measurements the concentration of an unknown amount of target can be determined, regardless of the variation in background fluorescence from the sample. In addition, the three measurements can be performed one after the other in a single tube. In addition to performing this work in buffer, experiments were extended to quantify transcription factors in cell extract solutions.

The goal of the work presented here is to extend these structure-switching aptamers to include a universal approach for creating this internal reference system with only three-steps for the quantification of various targets in additional complex solutions.

Chapter 2. Molecular Beacon Aptamer in a Tube

2.1 Introduction

Recent years have seen the development of a wide range of biosensors that employ binding-induced conformational changes in an oligonucleotide-based "receptor" to transduce molecular recognition events into easily detectable optical,[58] electrochemical,[59] microgravimetric,[60] or electronic[61] readouts. Examples include the use of DNA oligomers and aptamers attached to reporting agents such as Quantum Dots (QD),[62, 63] gold nanoparticles,[64, 65] gold surfaces,[66, 67] and fluorescent labels.[68] The advantages of these sensors include high specificity, low binding affinities, and quantitative detection, all while remaining wash-free and single-step. This suggests that they may prove promising as an approach to inexpensive, point-of-care molecular diagnostics.

Despite the potential advantages of beacon-type sensors, the use of these conformation-linked fluorescent sensors is complicated by the procedures needed to calibrate their response in complex sample matrices. For example, the background fluorescence arising from interferents and modulation of the beacon's fluorescence due to absorbance or quenching can vary from sample to sample and must be carefully corrected. Signal gain, the maximum signal that would be expected at saturating target, can likewise vary from experiment to experiment due to changes in the concentration of the beacon or sample conditions. Given these complications, beacon-type approaches rely on the use of sample blanks to determine baseline signals and the addition of saturating target to determine signal gain. Good blanks, however, can be difficult to obtain if, for example, patient-to-patient variations in blood composition are so significant that the blood of one subject cannot be used as an accurate blank for another. The use of saturating target to

determine a beacon's signal gain under authentic sample conditions can likewise be expensive or difficult depending on the target.

Here we demonstrate an approach to beacon calibration that employs three inexpensive reagents in a single-tube and three sequential measurements to achieve the quantitative determination of an unknown target in a complex sample matrix without the use of either blanks or saturating target.

2.1.1 General Approach

To determine the concentration of a target using a beacon requires knowledge of three experimental values. The first is the beacon's fluorescent output, F_{target} when it is in equilibrium with the target in the sample. We obtain this value by introducing the beacon to the sample, allowing the system to equilibrate, and then taking the first measurement. In order to correlate F_{target} with the occupancy of the beacon (from which, through its known disassociation constant, K_D, we can determine target concentration. We must also determine the signals observed when the beacon is entirely unoccupied in the same sample matrix, $F_{baseline}$, and when it is entirely occupied, $F_{saturation}$. To obtain the former we can "swamp" the system with a competitor that lacks the optical reporters and thus does not generate a signal upon target sequestration. The competitor can be comprised of either the same receptor at orders of magnitude higher concentration than the target or a higher affinity receptor in nearer stoichiometric excess. This competitor depletes the target molecules in the sample, allowing the measurement of $F_{baseline}$. To obtain $F_{saturation}$, in contrast, requires full occupancy of the beacon. This can be achieved via the addition of the target molecule in large excess over the beacon concentration and, if one is performing a single-tube

measurement, also over the concentration of the competitor. For many target molecules, however, this can be prohibitively expensive and/or inconvenient. In response we employ beacons that instead allosterically bind a specific "activator" oligonucleotide in a manner that mimics the conformational change associated with target binding. Our motivation for doing so is that oligonucleotide activators are generally less expensive and more convenient (stable and highly soluble) than many of the target molecules of interest.

Our approach to beacon-based concentration determination is reduced to three sequential fluorescence measurements in a single tube (Figure 2.1). First we add the beacon to the sample, equilibrate it with the endogenous target, and measure F_{target}. We then add an excess of competitor to this same tube, equilibrate again, and measure $F_{baseline}$. Finally, we add an excess of the activator, equilibrate a third time, and measure $F_{saturation}$. These three measurements are sufficient to calculate the target concentration as

$$[target] = \frac{K_D\,(F_{target} - F_{baseline})}{(F_{Saturation} - F_{target})} \qquad \text{Eq. 1}$$

where the K_D of the beacon under the comparable conditions has previously been determined. As you will see here, each system is dependent on the aptamer, however, the concentration ranges are 81x when the aptamer is under the determined K_D, and 10x when the aptamer is above the determined K_D, following the anticipated Langmuir isotherm.

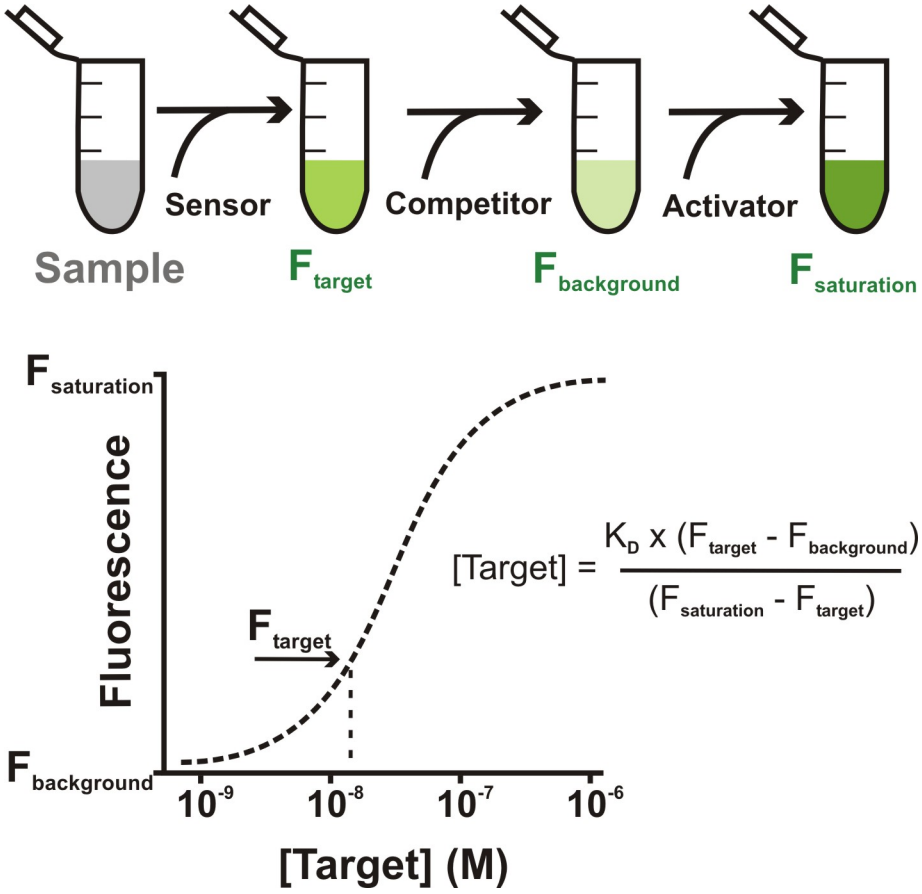

Figure 2.1 The three-step, single-tube calibration method for employing beacons in complex sample matrices. (Top) In the first step, the sensor is equilibrated with the target in the sample to determine F_{target}. Second, we add an excess of unlabeled competitor so as to de-populate the beacon-target complex, allowing us to measure $F_{baseline}$. Finally, the addition of an activator is used to simulate $F_{saturation}$, the fluorescence that would be observed were the beacon fully occupied. (Bottom) From these three measurements and the known disassociation constant of the beacon, K_D, we can derive the target concentration.

2.2 Results and Discussion

2.2.1 Molecular Beacon "Aptamer" as a First Model System

The first system with which we explored single-tube beacon calibration we employed the first reported sensor in this class, the “molecular beacon” of Kramer and co-

workers,[69] which is now commonly employed for the detection of specific DNA or RNA sequences.[70,71,72] Molecular beacons traditionally consist of a simple stem-loop DNA modified on its two ends with a fluorophore/quencher pair (Figure 2.2). In the absence of target the stem holds these optical reporters in close proximity, quenching fluorescence. Hybridization to a complementary target segregates the fluorophore from the quencher, increasing fluorescence. For our studies we fabricated a 27-base molecular beacon with a six base-pair stem, a tetramethylrhodamine carboxylic acid (TAMRA) fluorophore, and black hole quencher (BHQ). The loop of our molecular beacon recognizes 19 bases of a 23-base single-stranded target DNA. As a higher affinity competitor we employed a 27-base DNA lacking reporters and fully complementary to the target. Finally, as our activator we employed a 27-base DNA fully complementary to the molecular beacon, the binding of which mimics the binding of the authentic target.

Our single-tube calibration approach performs well when used with the molecular beacon in both simple buffers and more complex sample matrixes. To show this we first determined the beacon's disassociation constant to be 34.8 nM in 3-(N-morpholino)propanesulfonic acid (MOPS) buffer (10 mM MOPS, 140 mM NaNO3, 10 mM ethylenediamine tetra-acetic acid (EDTA), pH 7.4), and 23.7 nM in 50% fetal bovine serum in MOPS buffer (

Figure 2.3 and Figure 2.4). We then used our single-tube, three-measurement approach to determine the concentration of the beacon's target under both conditions. For example, starting with a known, 10 nM target concentration in MOPS buffer our three-measurement-one-tube approach recovers a concentration of 10.3 nM with a 95% confidence range of 8.5 to 12.2 nM. A second test run performed in 50% fetal bovine serum

(FBS) also using a 10 nM target concentration produced an answer of 9.1 nM with the 95% confidence range from 7.5 to 10.7 nM.

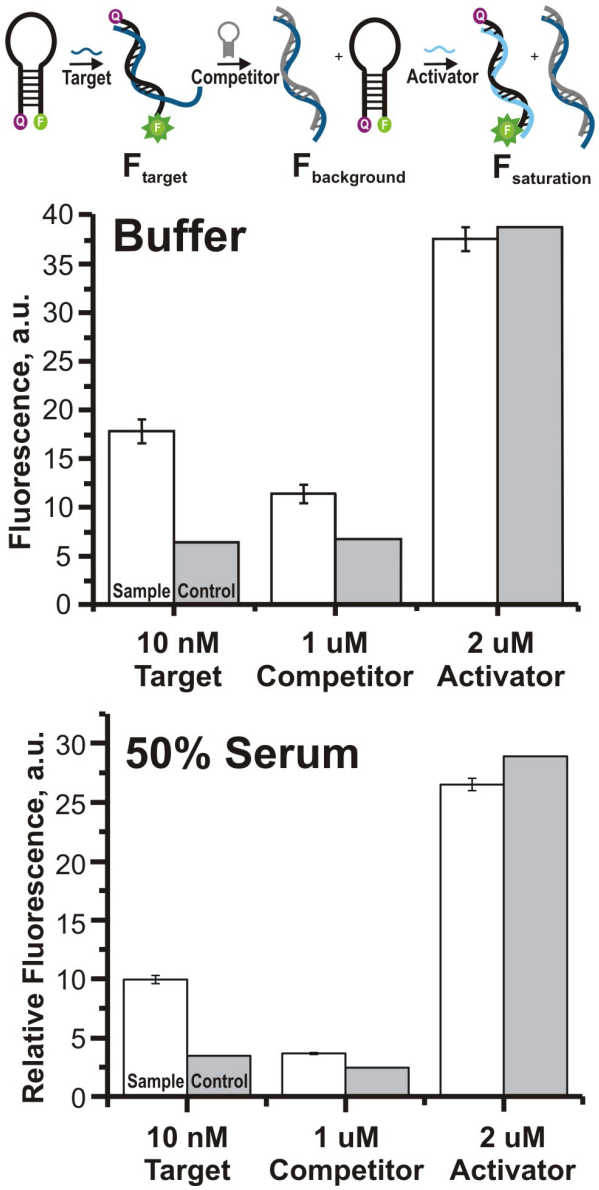

Figure 2.2 Single-tube calibration approach as applied to the measurement of the concentration of a specific nucleic acid sequence using a molecular beacon. (Top) From left, molecular beacon alone, before addition to the sample; upon target addition, target binds the beacon, opening the molecular beacon for fluorescence corresponding to concentration of target; addition of the competitor sequesters the target, allowing the molecular beacon to adopt the structure of no target present, or background signal; following these steps, the addition of activator saturates the beacon producing the maximum signal gain. (Middle) The response of the sensor in buffer with sample (white bars) or in a sample-free control (grey bars). Control solutions contain sensor but are not exposed to target. Control solutions are challenged with the activator in the last step to ensure the experimental saturation signals match that of a control. Calculated target concentration is 10.3 nM. (Bottom) The response of the sensor in 50% serum. Bars are the same colors as the middle graph. Calculated target concentration is 9.1 nM. All data points are the average value with error bars as standard error (n=3).

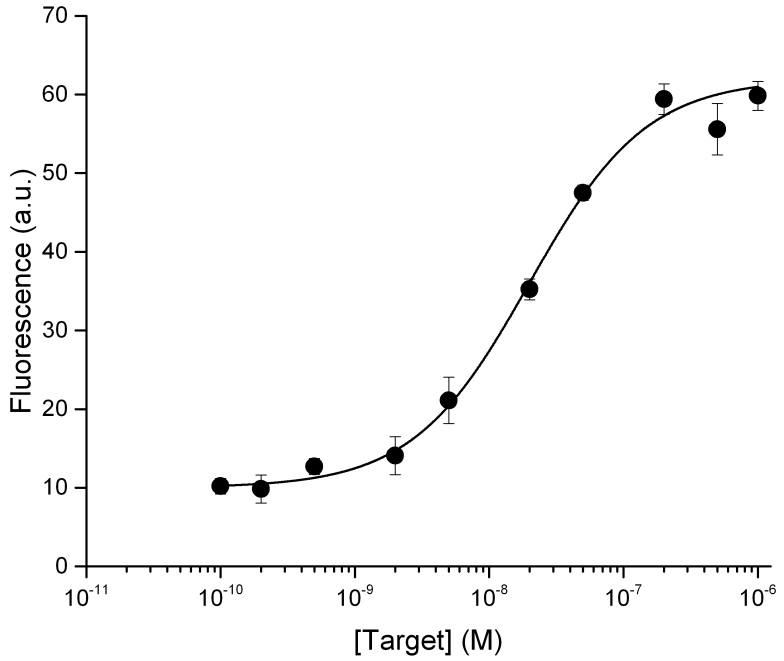

Figure 2.3 Titration of Molecular Beacon Aptamer sensor in MOPS Buffer. Data points are average and error bars are the standard error (n = 3). Langmuir isotherm fit is solid line.

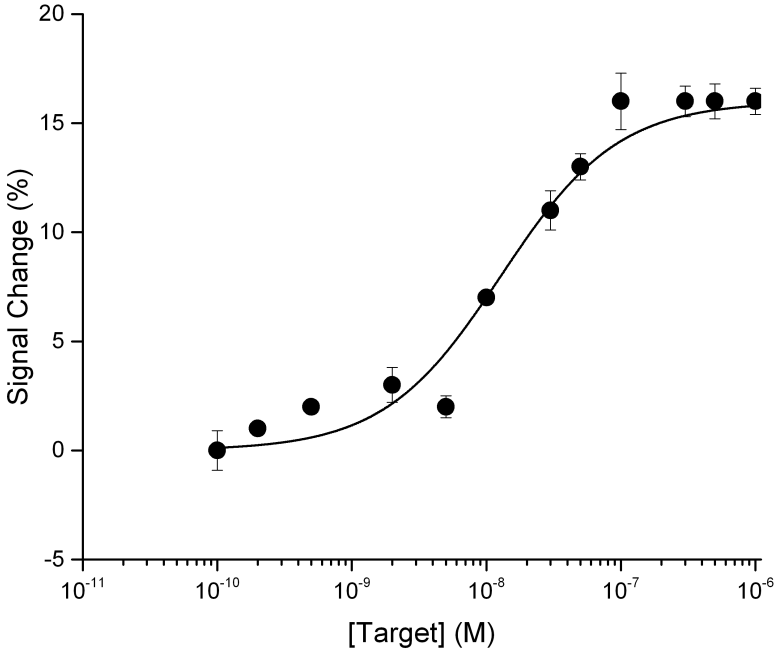

Figure 2.4 Titration of the molecular beacon sensor in 50% fetal bovine serum. Data points are average and error bars are the range (n = 2). Solid line is a Langmuir isotherm fit.

2.2.2 Silver-binding Aptamer

Expanding on the molecular beacon framework, Hamaguchi, Ellington and Stanton[73] were the first to report beacon-type sensors employing aptamer recognition elements – DNA or RNA molecules selected in vitro for their ability to detect specific non-nucleic acid targets – for the detection of proteins, small molecules and inorganic ions.[74,75,76] As a test bed to demonstrate the adaptation of our calibration approach to these more complex beacons we first employed a fairly simple aptamer that binds silver ions. Specifically, the silver ion binds between cysteine-cysteine mismatches in double stranded DNA,[77] an effect that has previously been used for the detection of this target.[78,79]

Elaborating on our modified molecular beacon we designed a beacon for the detection of silver and tested it in both simple buffer and in creek water samples. This 49-base beacon contains a fluorescein fluorophore, often abbreviated as FAM or FITC, at the 26th base, and a black hole quencher (BHQ) at its 5' end. In the absence of silver the beacon adopts a double-stem-loop structure that holds the fluorophore/quencher pair in proximity (Figure 2.5). Upon binding silver the beacon rearranges into a single-stem-loop structure that separates the pair. As the competitor we employed a 40-base pair stem loop containing 8 silver-binding C-C mismatches; because this does not undergo a binding-induced conformational change its affinity is significantly higher than that of the beacon. As an activator, we employ a 14-base element complementary to the 3' end of the beacon. Hybridization of the activator with the beacon opens the beacon in a manner that mimics the silver-bound conformation. However, when the activator is added, the beacon produces consistently lower fluorescence than saturating silver fluorescence. To correct $F_{saturation}$, the observed value is multiplied by 5/3. The disassociation constant of the beacon is 200 nM in

MOPS buffer and 51 nM in an environmental sample (creek water) diluted 50:50 with MOPS buffer (lowering the ionic strength alters the K_D) (Figure 2.6 and Figure 2.7). Using our one-tube three-measurement approach with a known target of 50 nM in MOPS buffer we recover a 46.6 nM silver ion concentration with a 95% confidence range of 39.7 to 53.4 nM. A second run using 50% creek water/50% MOPS buffer with a known target concentration of 20 nM recovers a concentration of 19.1 nM with a 95% confidence range of 11.2 to 27.1 nM.

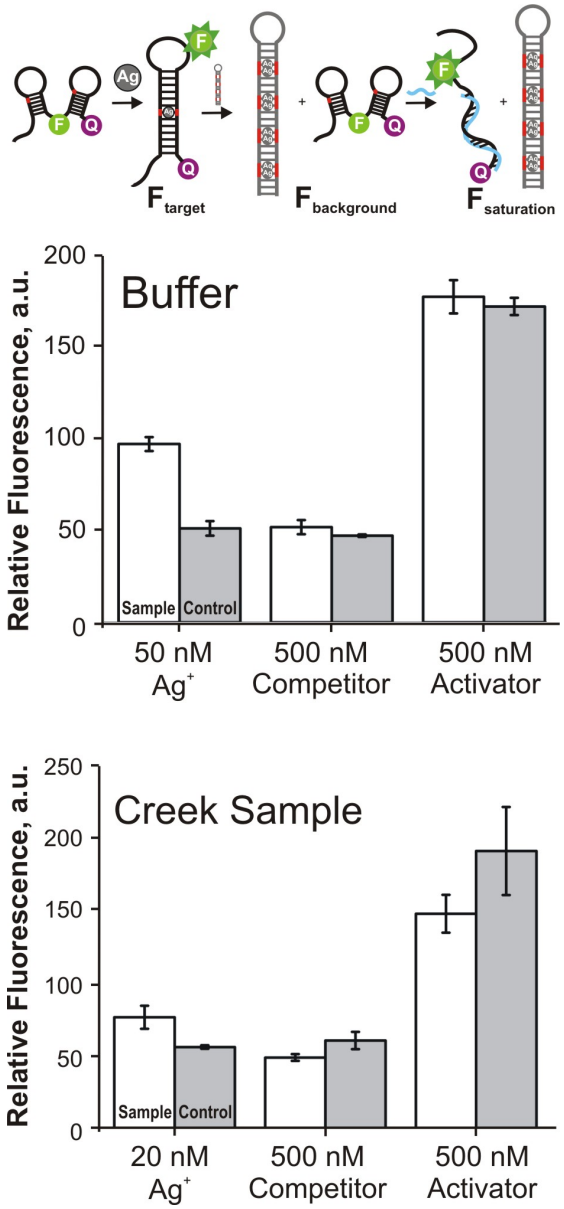

Figure 2.5 The measurement of silver ions using a beacon containing silver-binding C-C mismatches. (Top) Visual representation of the step-wise addition for the silver(I) ion detection system. From left, silver beacon alone, before addition to the sample; upon target addition, target binds the beacon, opening the two-stem architecture to a one-stem molecular beacon for fluorescence corresponding to concentration of target; addition of the competitor sequesters the silver ion, allowing the beacon to adopt the structure of no target present, or background signal; following these steps, the addition of activator binds to the beacon producing the maximum signal gain, equivalent to target saturation. (Middle) The response to sensor upon step-wise addition of the target in MOPS buffer. Bars in white are solutions exposed to samples, while grey bars are control solutions with sensor, but only exposed to activator to ensure replication. (Bottom) The response of the sensor upon step-wise addition of target in 50% creek sample. All data points are averages with error bars as standard error (n=3). Sensors were tested in creek water samples as silver(I) ion is toxic to fish in streams at levels above 2.5 nM, depending on fish species and size.[80, 81] .

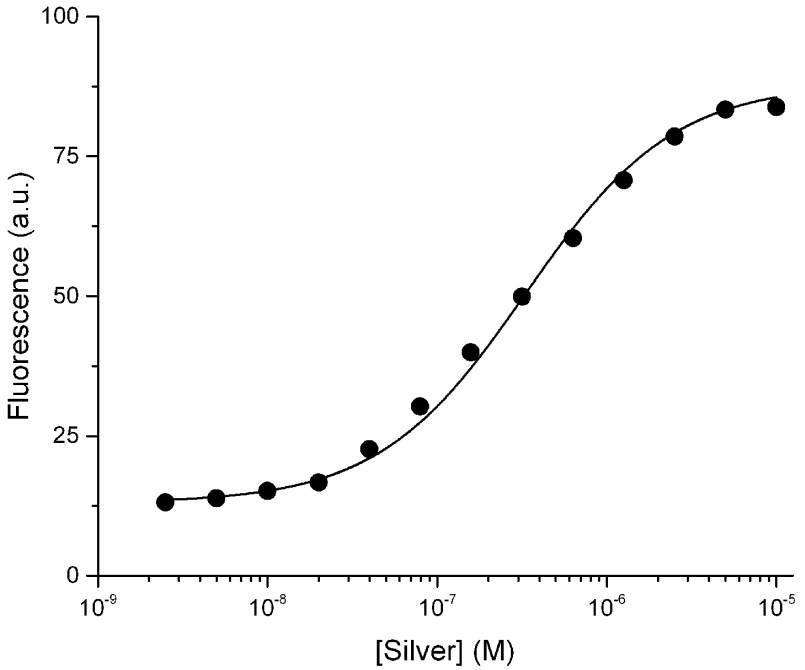

Figure 2.6 Titration of the silver ion sensor with silver ion in buffer. Data points are averages and error bars are standard errors (n=4). Error bars are obscured by data points. Solid line is Langmuir isotherm fit.

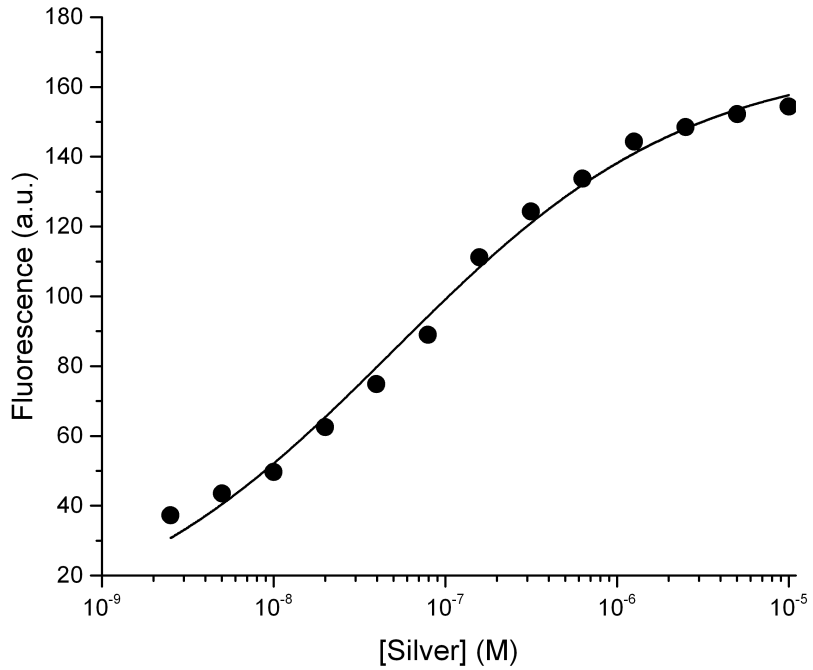

Figure 2.7 Titration of the silver ion sensor with silver ion in creek sample. Data points are averages and error bars are the range (n=2). Error bars are obscured by data points.Solid line is Langmuir isotherm fit.

2.2.3 Thrombin Aptamer

As a final test system we adapted our approach to the 15-base thrombin-binding aptamer of Hamaguchi, Ellington, and Stanton.[73] Here we added a 10-base tail to the 3' end of the aptamer such that the lengthened construct forms a stem-loop in the absence of target (Fig. 4). To determine the best location of the fluorophore for the best signal change upon thrombin binding, two architectures were created. The first, thrombin structure-switching aptamer 1 (TSSA1) has the fluorophore at its 5' end, and the quencher at the 3' end. The second, thrombin structure-switching aptamer 2 (TSSA2), was made with the fluorophore attached to thymine five bases from the 5' end, and retaining the quencher on the 3' end. Both aptamers fold into a molecular beacon, or stem-loop architecture, bringing the fluorophore/quencher pair into proximity. Upon thrombin binding the aptamer folds into a g-quadruplex, segregating this fluorophore/quencher pair, increasing fluorescence (Figure 2.8 and Figure 2.9). Indeed, the TSSA2 sensor, with a closer fluorophore/quencher pair, creates a larger change in signaling (Figure 2.10). Although this change is larger, the overall fluorescence is lower, most likely due to the close proximity of the pair, and may prove inhibitory upon use in serum. The experiments further detailed here all employ the architecture, named TSSA1, with the fluorophore at the 5' end of the sensor.

As competitor we employed the original 15-base aptamer with a 10 base poly-T tail. Thus the competitor does not form the stem-loop and possesses a higher affinity for thrombin than the beacon. As an activator we employ a 25-base construct complement to the full length of the beacon. Other lengths of activators were tested, however none proved to create the same saturating signal as the 25-base activator (Figure 2.11).

An investigation of this system revealed a K_D for the thrombin aptamer with human thrombin in buffer (10 mM Tris, 7.4 pH), of 16 nM (Figure 2.12). A singular experiment to determine an unknown concentration of thrombin was performed (Figure 2.13). From this experiment, the determined target concentration of 12 nM was significantly smaller than the spiked concentration of 20 nM thrombin. This experiment needs to be repeated in the future to determine accurate target concentrations.

Finally, in anticipation of challenging the system in blood serum, the sensor was tested against bovine thrombin. Although the aptamer was created to solely recognize the human thrombin, bovine thrombin is similar, differing by only few amino acids. Most importantly, there is only one amino acid different in the binding site of the aptamer. In Figure 2.14, increasing concentrations of bovine thrombin (bThrombin) are added to the sensor with some increase in fluorescence. As compared to the same sensor binding to human thrombin (hThrombin) however, the fluorescence increase is almost insignificant: hThrombin causes a 200% increase in signal while bThrombin only causes a 50% increase.

In future experiments, this three-step system must be completed. To fully complete the system as the molecular beacon and silver aptamer were completed, there are several required experiments. First, completing the stepwise sample concentration as described above with an accurate determination will allow the system to move forward to serum experimentation. While preparing the system for accurate target determination in serum solutions, any background bThrombin binding must be quantified. An experiment using the method of standard additions can quantify bThrombin in any fetal bovine serum before quantifying any spiked additions of hThrombin.

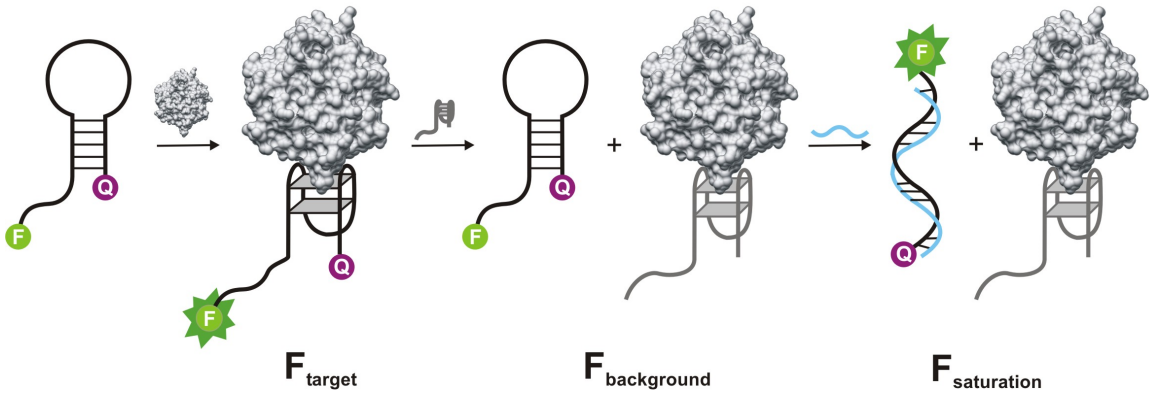

Figure 2.8 Measurement of thrombin protein with the thrombin aptamer. From left, thrombin beacon alone, before addition to the sample; upon thrombin addition, thrombin binds the sensor, opening the molecular beacon for fluorescence corresponding to concentration of target; addition of the competitor sequesters thrombin, allowing the beacon to adopt the structure of no target present, or background signal; following these steps, the addition of activator binds to the beacon producing the maximum signal gain, equivalent to thrombin saturation.

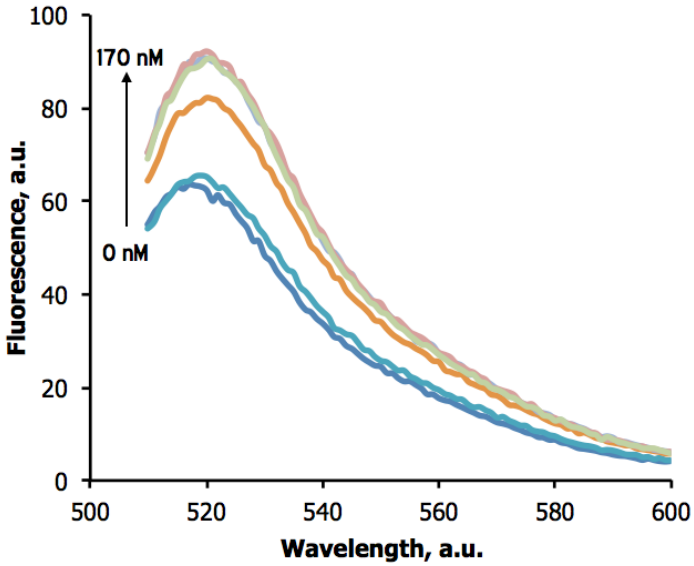

Figure 2.9 Titration of thrombin aptamer with hThrombin. This aptamer has the fluorophore on the 5' end with the quencher at the 3' end (TSSA1). Each scan is the average of 2 scans.

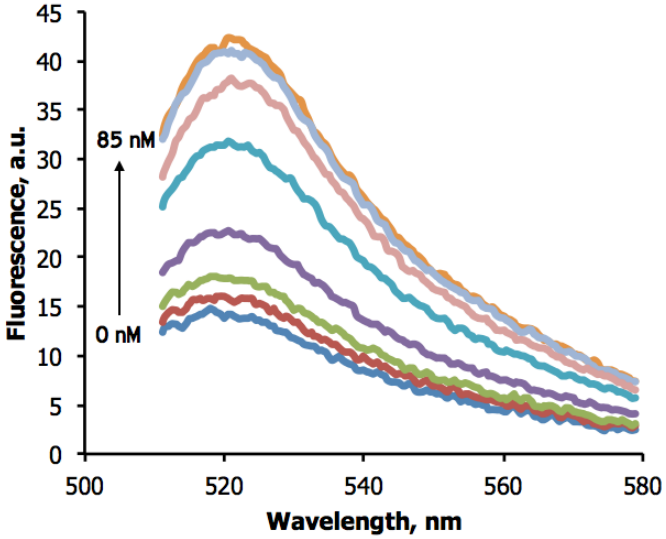

Figure 2.10 Titration of hThrombin with Thrombin Aptamer. This aptamer has the fluorophore inserted between the 5th and 6th base from the 5' end with the quencher at the 3' end (TSSA2). Each scan is the average of 2 scans.

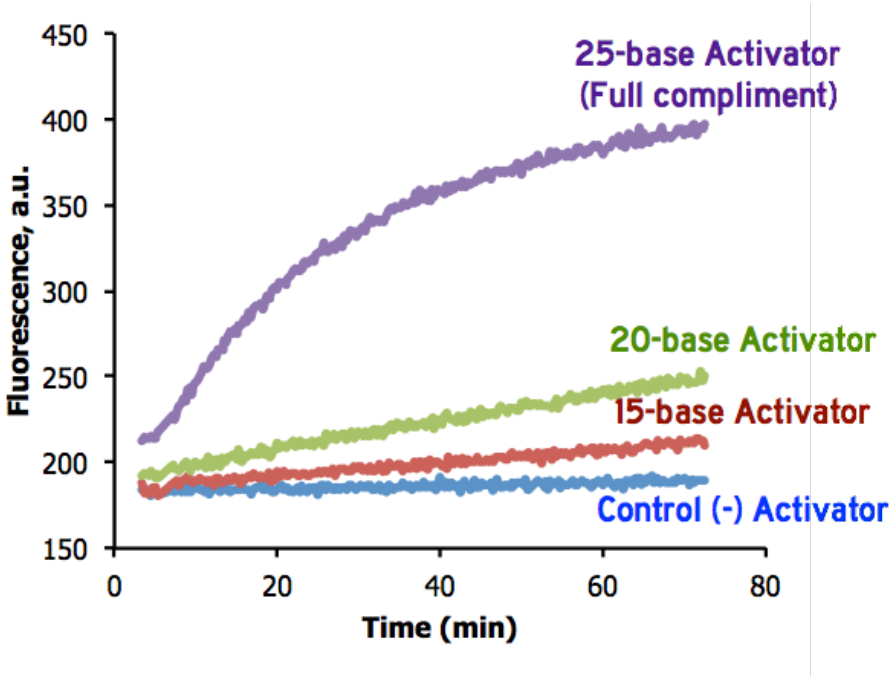

Figure 2.11 Time kinetics of various sized activators upon addition to the TSSA1 aptamer. Activators were added at 2 minutes, and data points were taken every 15 seconds.

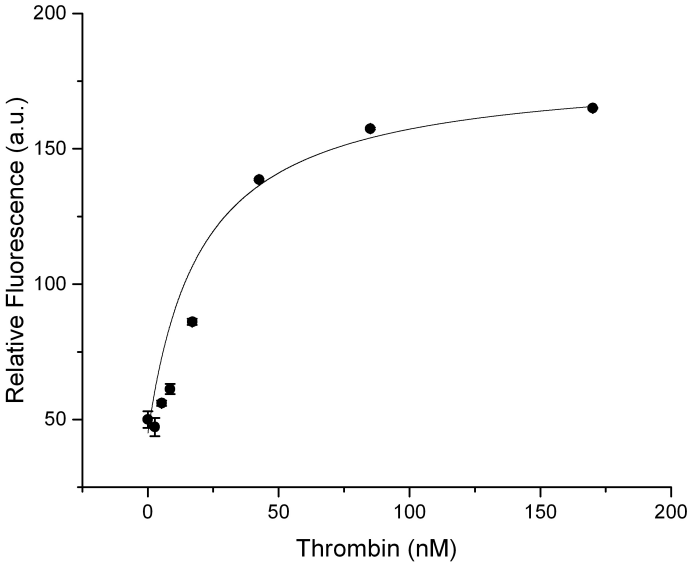

Figure 2.12 Titration of hThrombin with the Thrombin aptamer TSSA1. Data points are the average with error bars as the standard error (n=3). Fitted line is a Langmuir isotherm for K_D determination of 16 nM.

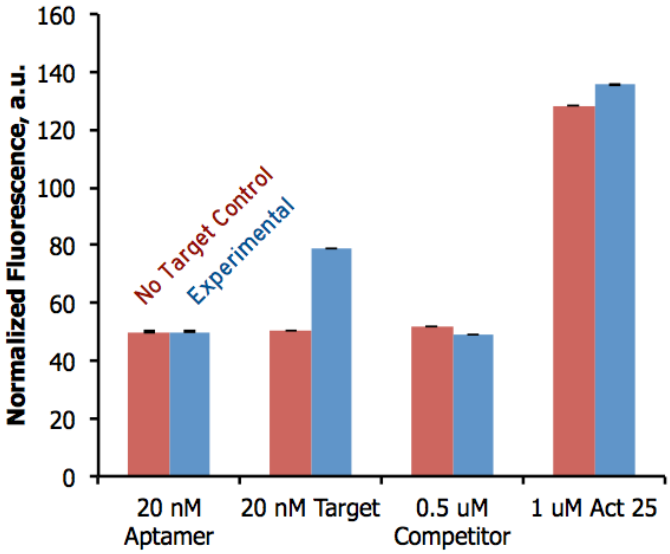

Figure 2.13 Concentration determination of hThrombin using the stepwise addition. Red bars indicate the control solutions with the TSSA1 aptamer with no target addition, but activator is added at the end. Blue bars indicate experimental solutions taken through the step-wise addition. All data bars are average with error bars as the range (n=2).

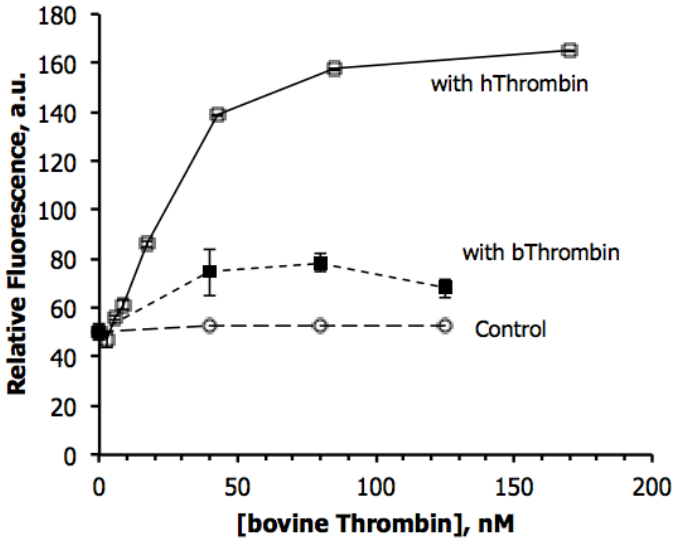

Figure 2.14 Titration of bThrombin and hThrombin with the Thrombin aptamer TSSA1. Data points reflect averages with error bars as the range (n=2).

As all projects go, not all perform optimally. The following examples were predecessors to the MBA, silver(I) ion, and thrombin aptamer systems. Each had its complications, from which lessons were learned to create the working three-step system. They are included in this thesis as documentation for future researchers.

2.2.4 PfLDH Aptamer

In beginning this project, the goal was to select an aptamer with relevance to the point-of-care world from literature. Additionally, the aptamer should have enough literature support to ensure repeatability and detail the location of aptamer binding to its target. These two requirements would allow for changes to the aptamer sequence with additions to create a structure-switching architecture.

This aptamer was found in the journal abbreviated *PNAS* with a co-crystallized structure of the protein and the created aptamer.[82] One appealing feature of this aptamer was its target, the lactose dehydrogenase protein from the malaria-causing protozoan parasite *Plasmodium falciparum* (PfLDH). The researchers determined that the aptamer detection of the malarial LDH was specific, and does not detect human LDH. A second appealing feature was the co-crystallization with the target molecule, providing an optimal way of tweaking the aptamer sequence with out reducing interactions between aptamer nucleotide bases and the protein.

While studying the aptamer-protein co-crystallization in the paper, the 27-base sequence important for binding forms a loose loop with some making hydrogen bonds. Additionally, the PfLDH protein is made of 4 subunits, with two aptamers binding between subunits A and B, and C and D. While studying the architecture of the aptamer, an important

flipped base at the 16th position (an adenine) from the 5' end shows interaction with the protein. Finally, the aptamer has an eight base sequence on the 3' end that could be used as a tail.

To create a structure-switching aptamer where the binding conformation turns fluorescence on, the loop that binds the protein must be hidden in the off state (Figure 2.15). To accomplish this, a tail on the 3' end of the aptamer binding sequence was created to bind the middle of the loop. This replaced the eight non-binding bases in the original aptamer. On each end of this newly created stem loop, a fluorophore and quencher were inserted into the sequence, such that fluorescence would be quenched in the non-binding form, and fluorescence would increase upon binding.

The final modification to the aptamer sequence added six bases on both the 3' and 5' ends of the sequence to act as toeholds for the stabilizer. Previously a stabilizer sequence held the sensor in the binding state with maximum fluorescence.[68]

Proteins PfLDH and human lactose dehydrogenase b (hLDHb) were acquired from the Tanner group, with frozen stock of PfLDH, and vectors for both PfLDH and hLDHb. Some primary experiments were performed using the frozen stocks of PfLDH while more protein was grown and purified.

The primary experiments showed decreases in fluorescence upon increasing PfLDH protein concentration. When challenged with a non-binding protein, bovine serum albumin (BSA), there was no change in fluorescence (Figure 2.16).

Upon analysis of the results along with the cartooned aptamer, it was determined that the fluorophore was interacting with the protein upon binding causing a decrease in fluorescence. Additionally, the initial fluorescence from the sensor suggested that the non-

binding state was not achieved such that the fluorophore and quencher were not in close enough proximity.

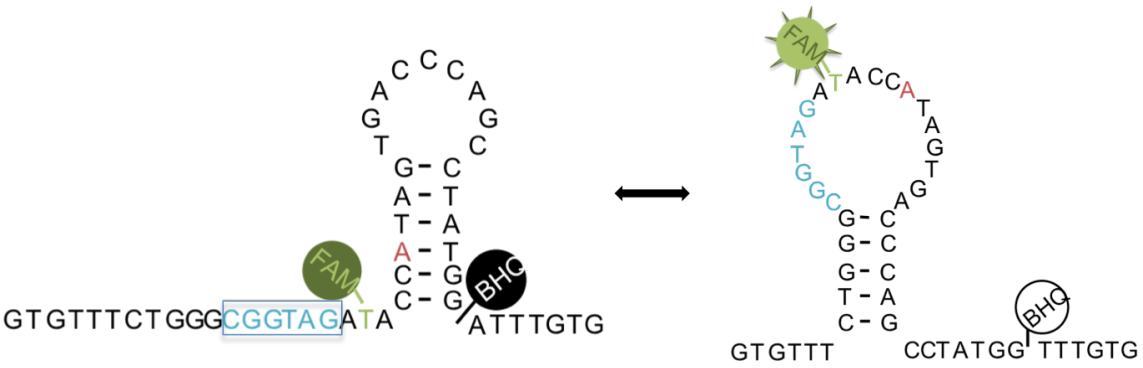

Figure 2.15 Cartooned structures of the PfLDH aptamer. 5' end is on left hand side in both drawings. Blue bases are the binding sequence to the protein. Red base is the flipped out base, also involved in binding. Fluorescein (FAM) is the fluorophore and BHQ is the black hole quencher. (Left) Nonbinding state, fluorophore and quencher pair are close in proximity. (Right) Binding state with the blue bases presented in the loop. Fluorophore and quencher pair are separated in this architecture, resulting in fluorescence.

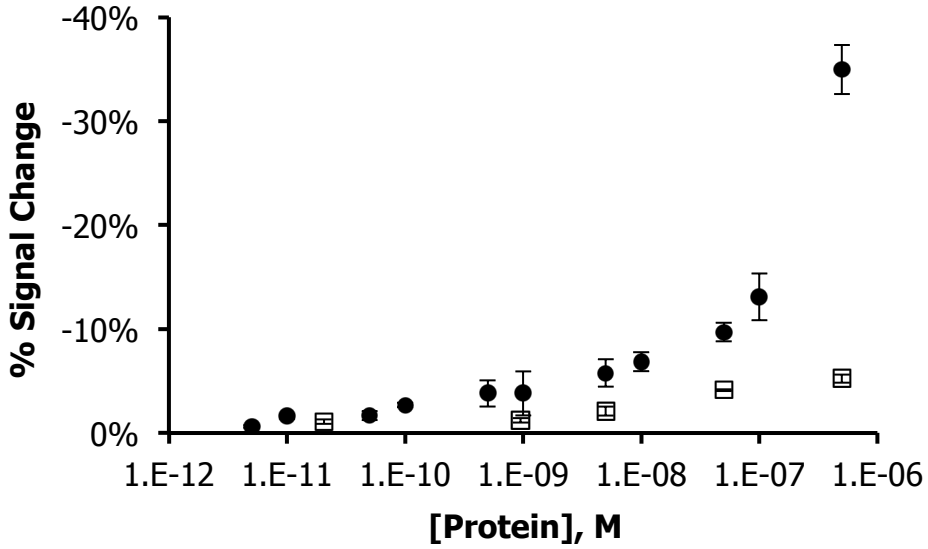

Figure 2.16 Titration of PfLDH aptamer with PfLDH protein and BSA as a negative control. Closed circles are challenged with PfLDH protein, open boxes are BSA challenged sensors. Data values are averages with error bars as standard deviation (n=3).

2.2.5 H6 Aptamer

After the PfLDH aptamer did not provide a pathway to a possible aptamer system, another aptamer was chosen from literature. The histidine tag aptamer was chosen from the Weihong Tan group, known for the development and use of aptamers. This aptamer targets the histidine tag added to the N terminus of proteins and was developed as a second generation in the Tan group from the original sequence patented in another form by Sharon Doyle and Michael Murphy.[83,84] The basis for choosing a histidine tag aptamer would also allow for detection of proteins within cell lysates. Although the aptamer would not be specific for a protein, it is rare to have more than one protein with a histidine tag within a bacterial culture, as this would not allow for purification. Here, I named the aptamer "H6 aptamer", for the six-histidine amino acids added to proteins as a tag for purification.

In the first experiments, the aptamer was challenged against the hLDHb protein. Since I personally prepared this protein, from growth through purification, it was a solid starting point. Additionally, the purification required a nickel column for the added his-tag. As seen in Figure 2.17, there was no change upon increasing amounts of hLDHb protein. A second protein, a commercially available his-tagged H1N1 recombinant protein was used to challenge the H6 aptamer. Due to the higher stock concentration, this protein allowed for a larger range of added his-tagged protein. As seen in Figure 2.18, the aptamer continued to not respond to known his-tagged proteins.

From these two negative responses to known histidine tagged proteins, this project was stopped. When looking retrospectively at this project, the aptamer did not have citations from other groups, which can reduce the aptamers reproducibility. Compared to the Tan group aptamer structure, the polyethylene glycol (PEG) spacer was removed, resulting in

possible higher rigidity and reduced ability of the aptamer to bind a histidine tag. All that said the original patented aptamer did not contain any spacers, so it is unlikely that the deletion of the PEG spacer caused the aptamer to detect his-tags.

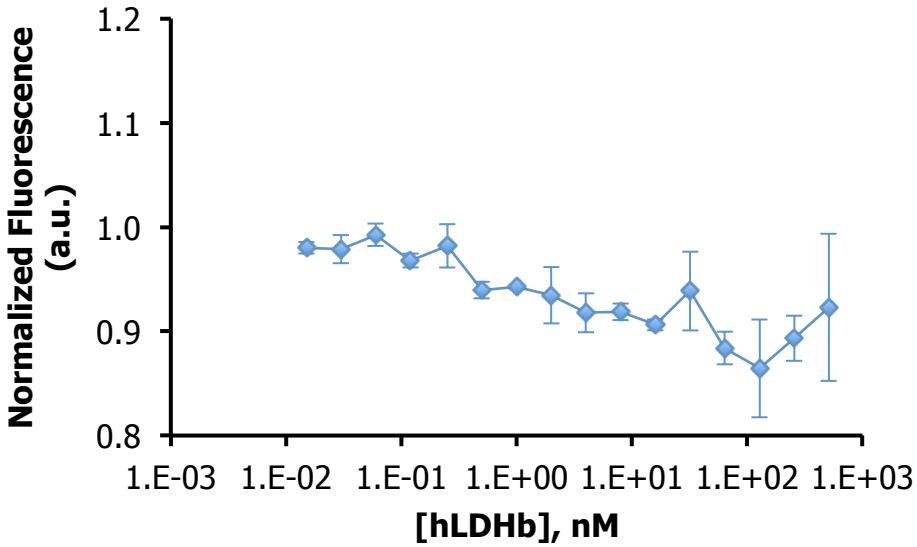

Figure 2.17 Titration of H6 aptamer with added hLDHb protein. Data points are averages and error bars are the range. (n=2).

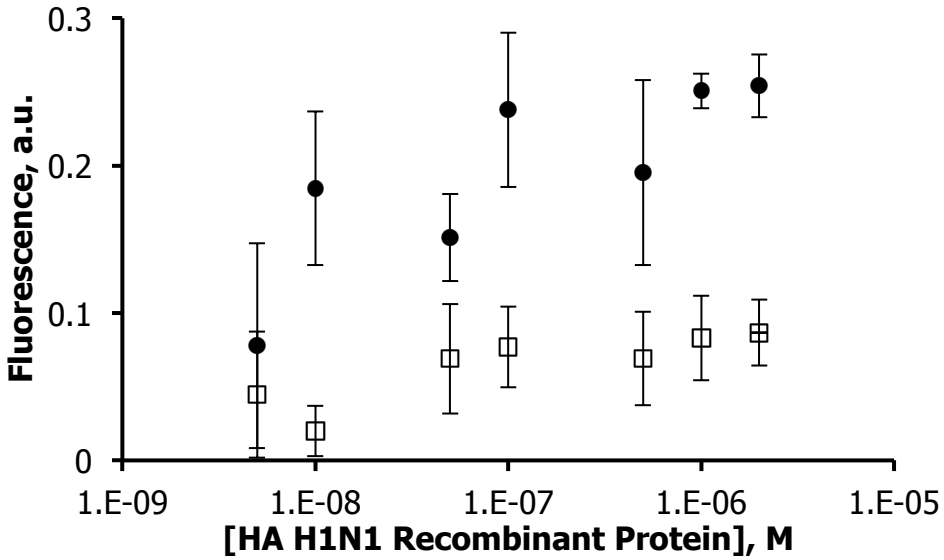

Figure 2.18 Titration of H6 aptamer with added H1N1 recombinant protein. Black circles are with the recombinant protein while the open squares are control solutions with no added target. Data points are averages and error bars are the range. (n=2)

2.2.6 Mercury Ion Aptamer

With two systems not working according to the goals of the project, literature was combed through to find aptamers used by at least two groups. The mercury(II) ion aptamer, or a thymine-thymine mismatch, had been used by many groups, including our own.[85,86,87] Instead of using the aptamer in a cooperative manner as many of the previous groups, a new sequence was produced with a singular thymine-thymine mismatch (Figure 2.19).

Upon completing many titrations, a problem arose at the higher concentrations of mercury chloride, a decrease in the overall fluorescence (Figure 2.20). Based on a literature search, heavy metals with f orbitals, such as mercury(II) could be interacting with the π orbitals of the fluorophore, and therefore acting as a quencher in solution. Even with lower concentrations titrated into solution, a plateau is not formed and rather decreases in fluorescence are seen, even at lower concentrations than when a wide concentration is performed (Figure 2.21). Further supporting this hypothesis of mercury (II) ion interfering with fluorescence was the addition of the mercury competitor, which caused a 20x increase in fluorescence. This increase in fluorescence could only be due to the capture of mercury ions in the competitor thymine mismatches, removing any interaction in solution to the fluorophore.

To also show that there is no quenching of fluorescence by heavy metals without f orbitals, silver (I) ion was added at increasing concentrations to a solution of the mercury aptamer (Figure 2.22). There was no decrease in fluorescence, instead however, there was an increase in fluorescence. With this knowledge, focus moved from the mercury ion aptamer to the silver ion aptamer.

Previous groups using the mercury aptamer were able to get around the quenching problem with mercury (II) due to the cooperativity of their sensors allowing for lower binding affinities. As we were interested in studying single binding events, this eliminated this sensor from being used in our project. We learned that heavy metals with f orbitals could contribute to fluorophore quenching at high concentrations.

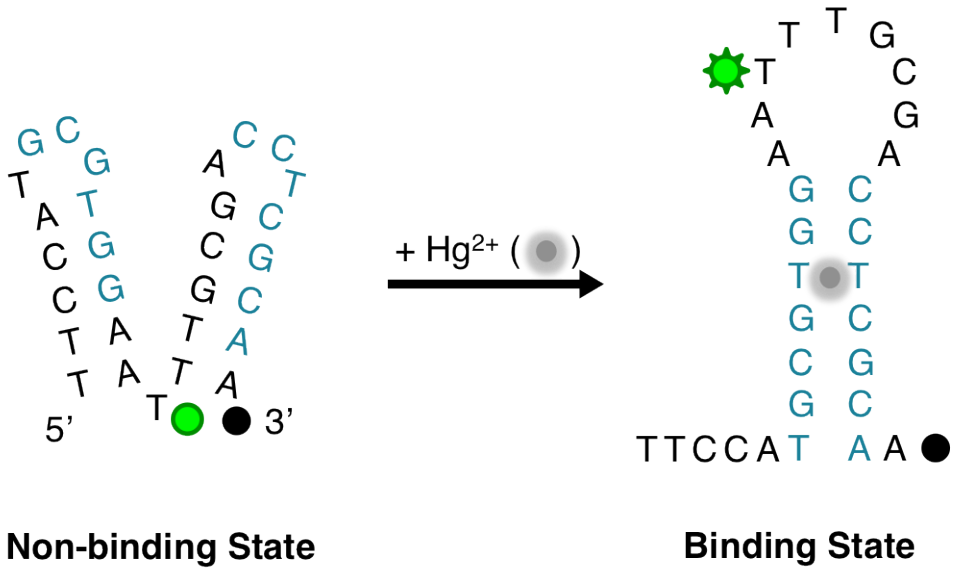

Figure 2.19 - Single mercury (II) ion molecular beacon aptamer. The non-binding state (left) is the energetically favorable state, and is kept in that state until mercury (II) ion is present. Sequence in blue shows the stem that forms in the presence of mercury (II) ion (right). Fluorescein is attached to the thymine (green circle), and onyx quencher A is at the 3' end (black circle).

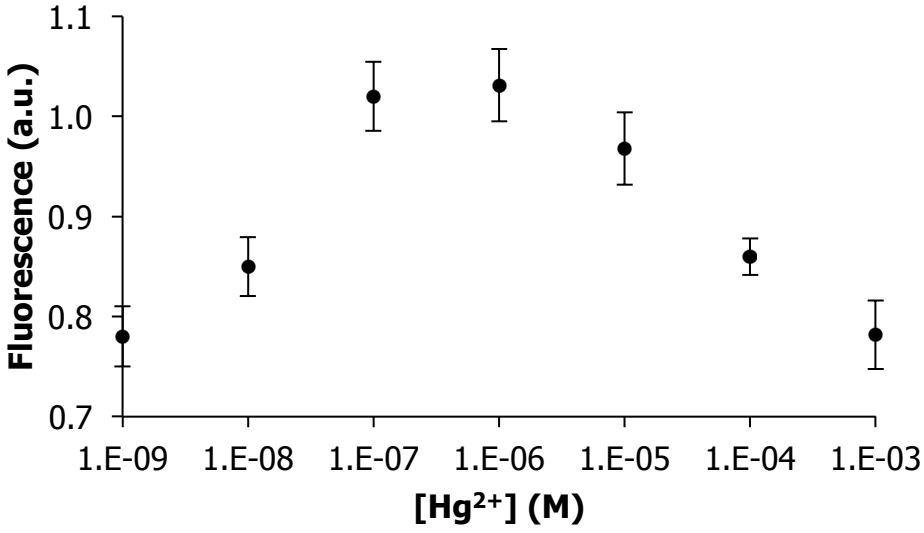

Figure 2.20 Titration of mercury(II) with 10 nM Mercury Aptamer. At higher concentrations of mercury, quenching is observed. Data points are averages with error bars as standard deviation (n=5).

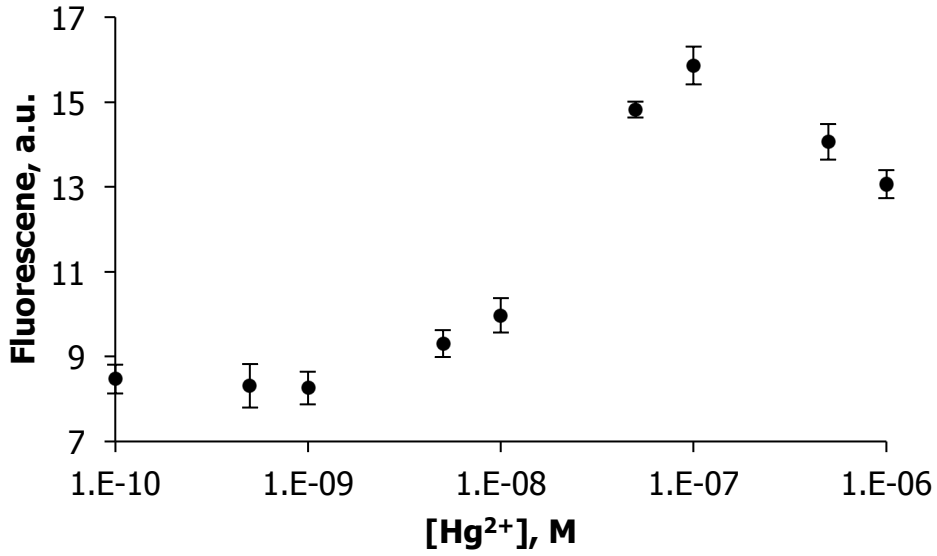

Figure 2.21 Titration of mercury (II) ion with mercury aptamer at lower concentrations. Decreases in fluorescence seen above 100 nM. Data points are averages and error bars are standard deviation (n = 3).

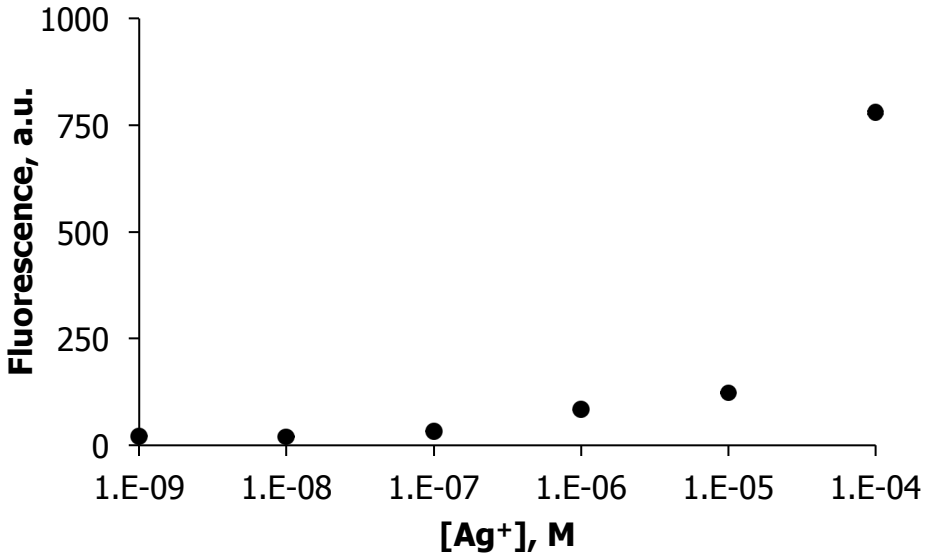

Figure 2.22 Titration of Silver (I) ion with the mercury aptamer as a demonstration that silver ion does not cause quenching. Data points are average with error bars as standard deviation (n = 5).

2.3 Conclusions

Here a novel approach has been described to perform calibrated molecular and aptamer beacon measurements. This approach is suitable for the quantification of targets even in complex sample matrices, which requires only three sequential measurements that are performed in a single tube. Further adding to its convenience, only inexpensive DNA-based reagents are required, obviating the need for the addition of saturating target to obtain an upper baseline for the measurements. I believe this technique can be universally applied to any target system, regardless of previous difficulties. The quantification of a target using this three-step system was proven through the detection of three different systems, a DNA strand, a small ion, and a protein.

Further work is necessary to completely show the thrombin aptamer works in serum samples. Although the groundwork and the path forward are provided, the experiments must be completed to fully show the aptamer working in the three-step system.

Should an additional aptamer be designed for the use in the three-step system, it is important to consider the binding of the aptamer to the target, the possibility of disrupting this binding with a second structure, and how an activator can be designed to mimic binding of the target at saturation. Serum has a high autofluorescence in the blue-green range, therefore, a fluorophore that excites in the red region will out-perform one in the green or yellow range. Furthermore, solution autofluorescence will be of great importance for future aptamer designs with the intention of using them in a complex solution.

2.4 Experimental

2.4.1 Materials

HPLC purified DNA sequences for MBA and mercury ion aptamers were ordered from Sigma-Aldrich (Woodbridge, MO), all other HPLC purified DNA sequences were ordered from Biosearch Technologies (Novato, CA). All DNA stock solutions were made to 100 μM using UltraPure distilled water (Gibco, Grand Island, NY; now Thermofisher Scientific) and stored at 4 °C in their original packaging. Mercury (II) chloride, silver perchlorate, 3-(N-morpholino)propanesulfonic acid (MOPS), BL21 (DE3) pLysS-T1 Competent Cells, and Fetal Bovine Serum (all from Sigma Aldrich, Saint Louis, MO), and sodium phosphate monobasic monohydrate, sodium phosphate dibasic monohydrate, LB Broth Muller, Acrylamide/bis-acrylamide 40% solution, ammonium persulfate (APS), N,N,N',N'-Tetramethylethylenediamine (TEMED), 10x Tris Borate EDTA (TBE) (made in house - Tris HCl, Boric Acid, imidazole, and sodium nitrate (all from Fisher Scientific, Fairlawn, NJ) were used as received. Additionally, an electrophoretic mobility shift assay (EMSA) kit (including EMSA dye, SYBR green, and SYPRO Ruby) (Life Technologies, now Thermofisher Scientific), ethylenediaminetetraacetic acid disodium salt dihydrate (EDTA), and silver nitrate (EMD Chemicals Inc., Gibbstown, NJ)), SOC Medium (Invitrogen, now Thermofisher Scientific), and human and bovine thrombin (Haematologic Technologies Inc., Essex Junction, VT) were used as received. A buffer solution of 140 mM 3-(N-morpholino)propanesulfonic acid (MOPS) and 10 mM sodium nitrate was pHed to 7.6 and filtered using Nalgene Rapid flow 0.2 μm nylon filters with 90 mm diameter (ThermoFisher Scientific, Waltham, MA) for experimentation.

2.4.2 Instrumentation

Fluorescence measurements were performed on a Cary Eclipse Fluorimeter (Varian, Mulgrave, Australia), gels were run in a Bio-Rad box using a Bio-Rad volt (Hercules, CA). pH measurements were performed with a VWR Symphony SB70P meter (Radnor, PA). Gels were imaged using a Typhoon Trio from GE Healthcare (Piscataway, NJ) or a Biorad Gel Doc XR+ System (Hercules, CA).

2.4.3 DNA sequences

All sequences are written from the 5' to 3' end.

<u>Molecular Beacon Set:</u>

Molecular Beacon (Aptamer): [6FAM] TGA CTC TAC CAA TGT GAA CGT GAG TCA [Onyx Quencher A]

MB Target (20 mer Activator): CTC AGT TCA CAT TGG TAG AG

MB Competitor: TGA CTC TAC CAA TGT GAA CGT GAG TCA

N Target (14 mer Activator w/ tail): CTC ACG TTC ACA TTT TAA CAG AT

N Competitor: AAA TCT GTT AAA ATG TGA ACG TGA GTT

<u>Silver Ion Set:</u>

Silver 1 Aptamer (Ag1): AAC CAA TGC CTG GTT [Fluorescein dT]TT GCG ACC ACG CAA [Onyx Quencher A]

Silver 1v2 Aptamer (Ag1v2): TAG TGT GCA ACG CTA GGA AGC GTT T[Fluorescein dT]T TTT TCC TAC CGT TGT AGG AAT G [Onyx Quencher A]

Silver 1v3 Aptamer (Ag1v3): GTA TAA TCG CGC TTA TA[Fluorescein dT] AAT TTG CCC GAA AAT TAG [Onyx Quencher A]

Silver Competitor: CGG CCT GAC CGC GCC GTA TTT TTA CCC CGC CCT CAC CCC G

Silver Full Activator:TTG CGT GGT CGC AAA AAC CAG GCA TTG GTT

Silver Activator 10 mer (Act 10): TTG CGT GGT C

Silver Activator 12 mer (Act 12): TTG CGT GGT CGC

Silver Activator 14 mer (Act 14): TTG CGT GGT CGC AA

Silver Activator 17 mer (Act 17): TTG CGT GGT CGC AAA AA

Silver Activator 19 mer (Act 19): TTG CGT GGT CGC AAA AAC C

Silver Activator 14 5':ATT CCT ACA ACG GT

Silver Activator 14 5' A7G: ATT CCT GCA ACG GT

Silver Activator 14 middle: GGT AGG AAA AAA AA

Silver Activator 14 middle A8G: GGT AGG AGA AAA AA

Silver 1v2 Stabilizer: CAT TCC TAC ACA CTA

Silver 1v3 Stabilizer: CAT ATT TTT AAT C

<u>Thrombin Structure Switching Aptamer Set:</u>

TSSA1: [Fluoroscein dT]TA TAT TAA CCA GGT TGG TGT GGT TGG [Onyx Quencher A]

TSSA2: TAT AT[Fluoroscein dT] AAC CAG GTT GGT GTG GTT GG[Onyx Quencher A]

OG Ellington TSSA: [FAM] CCA ACG GTT GGT GTG GTT GG [BHQ-1]

Competitor: TTT TTT TTT TTG GTT GGT GTG GTT GG

Activator 5: ATA TAT TTT T

Activator 8: TTA ATA TAT T

Activator 10: TGG TTA ATA T

Activator 15: CAA CCT GGT TAA TAT

Activator 20: CAC ACC AAC CTG GTT AAT AT

Activator 25: CCA ACC ACA CCA ACC TGG TTA ATA T

TAMRA TSSA1: [TAMRA] TAT ATT AAC CAG GTT GGT GTG GTT GG[BHQ-2]

PfLDH Aptamer Set:

PfLDH Aptamer: GTG TTT CTG GGC GGT AGA T(FAM)AC CAT AGT GAC CCA GCC TAT GG-BHQ-1 ATT TGT G

PfLDH Competitor with T: TTC TGG GCG GTA GAT ACC ATA GTG ACC CAG AA

PfLDH Competitor without T: TTC TGG GCG GTA GAA CCA TAG TGA CCC AGA A

Stabilizer: CAC AAA TCC ATA GGA AAC AC

Mercury (II) ion Set:

Mercury Aptamer: TTC CAT GCG TGG AA[Fluorescein dT] TTG CGA CCT CGC AA [Onyx Quencher A]

13 mer Activator: TTG CGA GGT CGC A

17 mer Activator: TTG CGA GGT CGC AAA TT

20 mer Activator: TTG CGA GGT CGC AAA TTC CA

Competitor: CGC GAT TTC CCT TTC CCT TTC CCT TTC CCG TTT TTA CGG GTT TGG GTT TGG GTT TGG GTT TTC GCG

H-6 Set:

3' Aptamer: CCT CAG ACA GGT TTG GTC TGG TTG G[BHQ-1]G TTT GGC TCC TGT GTA CGT [T-CAL Fluor Orange 560]CC AAA

5' Aptamer: CC[T-CAL Fluor Orange 560] CAG ACA GGT TTG GTC TG[BHQ-1] GTT GGG TTT GGC TCC TGT GTA CGT TCC AAA

Competitor: CGT ACA CAG GTT GGT CTG GTT GGG TTT GGC TCC TGT GTA CG

Stabilizer/Activator: TTT GGA ACG TAC ATT CTG AGG

2.4.4 Fluorescence Measurements

Measurements for the molecular beacon, mercury, and PfLDH, aptamers with FAM dye were taken with excitation of 495 (± 5) nm and emission of 515 (± 10) nm with an average acquisition time of 0.5 s using a fluorescence cuvette from Starna Cells (Atascadero, CA). Measurements for the molecular beacon aptamer with TAMRA dye were taken with excitation of 550 (± 5) nm and emission of 580 (± 5) with an average acquisition time of 0.5 s using the same quartz fluorescence cuvettes. Measurements for mercury (II) ions were performed in disposable fluorescence cuvettes from VWR (Radnor, PA). The MBA, mercury (II) ion, PfLDH, and H6 aptamer systems collected data using the Kinetics program from Varian with measurements taken every 0.2 min. Aptamers were used at 2 nM, with the activator and competitor added to the same tube at 2 uM.

For the silver (I) ion and Thrombin Aptamer systems, scanning measurements were performed to determine any shift in the fluorescence emission peak. Excitation measurements of 495 (± 5) and an emission scan of 510 – 660 nm for FAM dye, or an

excitation of 560 (± 5) nm and emission scan of 575 – 660 (± 5) nm for TAMRA dye were utilized. Consistently across experiments measurements were performed with a scanning rate of 300 nm/min, an average acquisition time of 0.2 s and data acquisition every 1.0 nm.

For the three-step calibration method for target determination experiments, either aptamer or target could be added to the blank solution as the first step. Followed by the addition of either target or aptamer (whichever had not previously been added). Upon equilibration, the competitor is then added, with another equilibration, and finally the activator is added and equilibrium established. For the molecular beacon, working concentrations of 2 nM for probe, 2 uM for competitor, and 2 uM for activator were used. Silver(I) probe used 10 nM of probe, 500 nM competitor, and 500 nM activator. Thrombin probe used 40 nM probe, 500 nM competitor, 500 nM activator.

All measurements, for either the determination of the disassociation constant or target concentration, included a control of probe only with no target added. Experiments were performed using the temperature control at 20 °C. Control solutions always included an addition of the activator to ensure equal saturation before and after target addition.

2.4.5 Data Analysis

Data collected with the kinetics program.

The last five data points were averaged for the reported data point. If there were multiple cuvettes for a data point the averages were performed for all of the last five data points. Therefore if there were two cuvettes, ten points would be averaged, five from one cuvette, and five from the other.

Data collected with the scan program.

The background, or blank, scan was subtracted from all scans at a wavelength-by-wavelength subtraction. The lambda max was determined with the target or activator scan, and this was used across all scans. At the lambda max, an average was performed of the max +/- 2 nm. This average was used as the data point. If there were multiple cuvettes for a data point, the averages were averaged, and the standard error was taken from the averages only.

2.4.6 Gel Electrophoresis

Sodium dodecyl sulfate polyacrylamide gel electrophoresis (SDS PAGE) gels were created by hand. The stacking portion of the gel was created using 3.07 mL diH_2O, 1.25 mL 1.0 M Tris HCl, 0.025 mL 0.5 % (w/v) SDS, 0.67 mL Acrylamide-bis (40:0.8), 0.025 mL Ammonium persulfate (APS), and 0.005 mL TEMED. The running portion was prepared using 10.2 mL diH_2O, 7.5 mL 1.0 M Tris HCl, 0.15 mL 0.5 % (w/v) SDS, 12.0 mL Acrylamide-bis (40:0.8), 0.15 mL APS, and 0.02 mL TEMED. The running gel was first added to three-quarters of the gel mold, and water was added on the top to create a flat surface. After the gel polymerized, the water was poured off and the stacking portion was added to the top quarter, and the lane comb was added.

Samples were prepared with sample buffer (10 % (w/v) SDS, 10 mM DTT, 20 % Glycerol (v/v), and 0.2 M Tris HCl), and heated to 95 °C for 10 minutes. After loading samples, gels were run at 180 V for 30 minutes with a running buffer of 25 mM Tris HCl, 200 mM glycine, and 0.1 % (w/v) SDS.

2.4.7 Protein Transfection

E. Coli BL21 (DE3) pLysS-T1R competent cells were transfected with plasmids for *Plasmodium falciparium* lactase dehydrogenase (PfLDH) and human lactase dehydrogenase (hLDHb) proteins using the protocol from Sigma-Aldrich. Briefly, cells, plasmids, and control DNA were removed from -80 °C storage and allowed to thaw on crushed ice for 5 min. Control DNA was added to one tube of cells by adding 1 uL of cells and flicking the tube to mix then returned to ice. The PfLDH vector (at 29 ug/uL) was added to 2 tubes at 50 ng/tube, and the hLDHb vector (at 9.5 ug/uL) was added to 2 tubes at 50 and 40 ng/tube respectively. Cells were incubated on ice for 30 minutes followed by heat shock at 37 °C in a water bath for 45 seconds and returned to ice for 2 minutes. Super Optimal broth with Catabolite reduction (SOC) medium was added to the cell tubes at 450 uL then the solutions were transferred to culture tubes and incubated at 42 °C with shaking at 230 rpm for an hour. Cell solutions were spread on kanamycin LB agar plates at 30, 60, and 90 uL per plate. Once dry, plates were incubated overnight in the warm room at 42 °C.

Plates were determined to not have grown any cultures resulting from failed transfection. The liquid cultures were used again on plates, as the cultures were kept at 4 °C and parafilmed after use. Only hLDHb showed growth and three colonies were selected for growth overnight in liquid cultures. Cultures were split 1:50 for 100 mL growths and grown until $OD_{600} = 0.5$. Glycerol stocks were made for future use, while additional cultures were incubated overnight for vector miniprep.

A StrataPrep Plasmid Miniprep kit (Stratagene) was used to retrieve plasmid DNA for sequencing; procedures were followed and described briefly here. Cultures were spun at 15,000 rpm for 30 seconds to pellet and the supernatant was discarded. Multiple spindowns

were performed to get most of the supernatant off the sample. Cells were lysed using a stepwise addition of chemical 1, and cells were re-suspended by vortexing, followed by additions of Chemical 2 and Chemical 3. Supernatant was removed after spinning for 5 minutes and transferred to a microspin cup and spun for 30 seconds. Nuclease removal buffer was washed through the sample followed by wash buffer. The filtrate was kept and concentrations were found using the nanodrop; culture 1 was 89 ng/uL, culture 2 was 72.1 ng/uL and culture 3 was 50 ng/uL. These samples were stored at -20 °C.

The University of California Berkeley DNA Sequencing Facility sequenced samples. A total of 0.5 ug of cultures 1 and 2 were sent for processing. Culture 3 did not have a high enough concentration for sequencing. Results of the sequencing are shown in Figure 2.23. Additional tubes were left at -80 °C.

2.4.8 Protein Purification

Frozen stocks of clone 2 were pulled from the -80 °C freezer and 325 uL of the cells were added to 5 mL of LB with 35 mg/mL kanamycin. Tubes were incubated at 42 °C at 201 rpm for 20 hours. Cells were split at 1:100 and grown for 3.5 hours to achieve an OD_{600} of 0.51. IPDG was added at 0.5 mM to induce high protein production. Cells were incubated for an additional 4 hours then pelleted for 30 minutes at 5,000 rpm (2400 – 4400 x g), the supernatant was poured off and pellets were refridgerated overnight at 4 °C.

A lysis buffer (50 mM Tris HCl, 0.3 M NaCl, 20 mM imidazole, pH 7.5, SigmaFast Protein Inhibitor, >250 U benzonase) was added to the pellets, swirled, and let sit on ice for 30 minutes. Pellets were re-dissolved using swirling and vortexing. Ultimately cells were lysed by sonication in a water bath. Lysed cells were transferred to centrifuge tubes for

pelleting at 14,000 rpm for 20 minutes. Pellets were kept as a control, and supernatant was loaded onto a GE Healthcare His-trap crude column (1 mL). After loading the supernatant, it was allowed to interact with the column for 1.5 hours before performing a wash (HK Buffer: 25 mM Tris HCl, 0.1 M NaCl, 20 mM Imidazole, pH 7.5) of 40 mL and letting sit for an additional hour.

The column was eluded with 5 column equivalents (5 mL) each of increasing concentrations of imidazole in HK buffer. The four concentrations were 50, 100, 250, and 500 mM imidazole total in HK buffer (instead of 20 mM). Each of these increasing concentrations were considered a fraction, with the last imidazole concentration split into 5 fractions of 1 mL each. Each fraction was measured using UV/Vis spectroscopy at wavelengths of 260, 280, and 320 nm. Protein concentration was determined using the equation:

$$[protein] = 1.55(\lambda_{280}) - 0.76(\lambda_{260}) \qquad \text{Eqn. 3}$$

Samples with concentrations above 0.2 were considered to have the protein hLDHb in high and pure enough concentrations.

SDS-PAGE gel was performed on the fractions to confirm the contents of the fractions. As compared to provided PfLDH, approximately the same MW as hLDHb, fractions 4-11 have the same MW, but have two bands, one in a distinctly higher molecular weight band than the expected LDH band.

Fractions 6 – 11 were pooled (~10 mL) and concentrated using a 3 KDa MW cutoff spin method for 20 minutes at 2400 x g. Fractions 4 and 5 were not included as they did not contain any protein according to the spectroscopy analysis. After this concentration, the

concentrated portion was transferred to another concentrator with 30,000 Da cutoff and spun for 20 minutes at 2400 x g 4x to obtain ~ 1 mL of concentrated protein. This protein was stored at -20 °C and used in experiments with his-tags and for PfLDH experiments.

The concentrated protein was then dialyzed using a Thermo-fisher slyde-a-lyzer dialysis cassette with a 3500 MW cutoff for volumes of 0.5 – 3.0 mL to remove excess imidazole. Dialysis was performed with HK buffer for 3 hours, and then buffer was exchanged for fresh, and left for 48 hours.

```
hLDH        MATLKEKLIAPVAEEEATVPNNKITVVGVGQVGMACAISILGKSLADELALVDVLEDKLK
Clone1      MATLKEKLIAPVAEEEATVPNNKITVVGVGQVGMACAISILGKSLADELALVDVLEDKLK
Clone2      MATLKEKLIAPVAEEEATVPNNKITVVGVGQVGMACAISILGKSLADELALVDVLEDKLK
            ************************************************************

hLDH        GEMMDLQHGSLFLQTPKIVADKDYSVTANSKIVVVTAGVRQQEGESRLNLVQRNVNVFKF
Clone1      GEMMDLQHGSLFLQTPKIVADKDYSVTANSKIVVVTAGVRQQEGESRLNLVQRNVNVFKF
Clone2      GEMMDLQHGSLFLQTPKIVADKDYSVTANSKIVVVTAGVRQQEGESRLNLVQRNVNVFKF
            ************************************************************

hLDH        IIPQIVKYSPDCIIIVVSNPVDILTYVTWKLSGLPKHRVIGSGCNLDSARFRYLMAEKLG
Clone1      IIPQIVKYSPDCIIIVVSNPVDILTYVTWKLSGLPKHRVIGSGCNLDSARFRYLMAEKLG
Clone2      IIPQIVKYSPDCIIIVVSNPVDILTYVTWKLSGLPKHRVIGSGCNLDSARFRYLMAEKLG
            ************************************************************

hLDH        IHPSSCHGWILGEHGDSSVAVWSGVNVAGVSLQELNPEMGTDNDSENWKEVHKMVVESAY
Clone1      IHPSSCHGWILGEHGDSSVAVWSGVNVAGVSLQELNPEMGTDNDSENWKEVHKMVVESAY
Clone2      IHPSSCHGWILGEHGDSSVAVWSGVNVAGVSLQELNPEMGTDNDSENWKEVHKMVVESAY
            ************************************************************

hLDH        EVIKLKGYTNWAIGLSVADLIESMLKNLSRIHPVSTMVKGMYGIENEVFLSLPCILNARG
Clone1      EVIKLKGYTNWAIGLSVADLIESMLKNLSRIHPVSTMVKGMYGIENEVFLSLPCILNARG
Clone2      EVIKLKGYTNWAIGLSVADLIESMLKNLSRIHPVSTMVKGMYGIENEVFLSLPCILNARG
            ************************************************************

hLDH        LTSVINQKLKDDEVAQLKKSADTLWDIQKDLKDL
Clone1      LTSVINQKLKDDEVAQLKKSADTLWDIQKDLKDL
Clone2      LTSVINQKLKDDEVAQLKKSADTLWDIQKDLKDL
            **********************************
```

Figure 2.23 Sequence alignment of human LDH b with two different transfection colony clones. The asterisks under the alignment show an exact match.

This chapter in part adapted from:

Kallewaard-Lum, H.M., Larisch, M., and Plaxco, K.W. **2016.** "A single-tube, three-measurement approach to calibrated beacons using DNA structure switching aptamers in complex samples." *In Preparation.*

Chapter 3. References

[1] Scott, J.D., and Gretch, D.R. **2007**. "Molecular diagnostics of hepatitis C virus infection: a systematic review." *Journal of the American Medical Association*, **297**, 724-732.

[2] Tang, Y.W., Procop, G.W., and Persing, D.H. **1997**. "Molecular diagnostics of infectious diseases." *Clinical Chemistry*, **43**, 2021-2038.

[3] Brennan, D.J., O'Connor, D.P., Rexhepaj, E., Ponten, F., and Gallagher, W.M. **2010**. "Antibody-based proteomics: fast-tracking molecular diagnostics in oncology." *Nature Reviews Cancer*, **10**, 605-617.

[4] Evans, W.E., and Relling M.V. **1999**. "Pharmacogenomics: Translating Functional Genomics into Rational Therapeutics." *Science*, **286**, 487-491.

[5] Barany, F. **1991**. "Genetic disease detection and DNA amplification using cloned thermostable ligase." *Proceeding of the National Academy of the United States of America*, **88**, 189-193.

[6] Bennett, P.R., Le Van Kim, C., Colin, Y., Warwick, R.M., Chérif-Zahar, B., Fisk, N.M., and Cartron, J.P. **1993**. "Prenatal determination of fetal RhD type by DNA Amplification." *New England Journal of Medicine*, **329**, 607-610.

[7] Chen, X., Ba, Y., Ma, L., Cai, X., Yin, Y., Wang, K., Guo, J., Zhang, Y., Chen, J., Guo, X., Li, Q., Li, X., Wang, W., Zhang, Y., Wang, J., Jiang, X., Xiang, Y., Xu, C., Zheng, P., Zhang, J., Li, R., Zhang, H., Shang, X., Gong, T., Ning, G., Wang, J., Zen, K., Zhang, J., and Zhang, C.Y. **2008**. "Characterization of microRNAs in serum: a novel class of biomarkers for diagnosis of cancer and other diseases." *Cell Research*, **18**, 997-1006.

[8] Petricoin, E.F., Belluco, C., Araujo, R.P., Liotta, L.A. **2006**. "The blood peptidome: a higher dimension of information content for cancer biomarker discovery." *Nature Reviews Cancer*, **6**, 961-967.

[9] Eisenstein, B.I. **1990**. "The Polymerase Chain Reaction – A New Method of Using Molecular Genetics for Medical Diagnosis." *New England Journal of Medicine*, **322**, 178-183.

[10] Klein, D. **2002**. "Quantification using real-time PCR technology: applications and limitations." *Trends in Molecular Medicine*, **8**, 257-260.

[11] Manor, P.G. **1999**. "Turnaround times in the laboratory: a review of the literature." *Clincal Laboratory Science*, **12**, 85-89.

[12] Hawkins, R.C. **2007**. "Laboratory Turnaround Time." *Clinical Biochemistry Reviews*, **28**, 179-194.

[13] Gage, J.C., Ferreccio, C., Gonzales, M., Arroyo, R., Huivín, M., and Robles, S.C. **2003**. "Follow-up care of women with an abnormal cytology in a low-resource setting." *Cancer Detection and Prevention*, **27**, 466-471.

[14] Yager, P., Domingo, G.J., and Gerdes, J. **2008**. "Point-of-Care Diagnostics for Global Health." *Annual Review of Biomedical Engineering*, **10**, 107-144.

[15] Wide, L., and Gemzell, C.A. **1960**. "An Immunological Pregnancy Test." *Acta Endocrinology*, **35**, 261-267.

[16] Williams, D.L., Doig Jr., A.R., and Korosi, A. **1970**. "Electrochemical-enzymatic analysis of blood glucose and lactate." *Analytical Chemistry*, **41**, 118-121.

[17] Heller, M.J. **2002**. "DNA Microarray Technology: Devices, Systems, and Applications." *Annual Review of Biomedical Engineering*, **4**, 129-153.

[18] Chang, T-W. **1983**. "Binding of cells to matrixes of distinct antibodies coated on solid surface." Journal of Immunological Methods, 65, 217-223.

[19] Chinnasamy, T.; Segerink, L.I.; Nystrand, M.; Gantelius, J.; Svahn, H.A. A lateral flow paper microarray for rapid allergy point of care diagnostics. Analyst 2014, 139, 2348-2354.

[20] Buchegger, P.; Sauer, U.; Toth-Székély, H.; and Preininger, C. Miniaturized Protein Microarray with Internal Calibration as Point-of-Care Device for Diagnosis of Neonatal Sepsis. *Sensors* **2012**, *12*, 1494-1508.

[21] Hansen, R.R.; Johnson, L.M.; and Bowman, C.N. Visual, base-specific detection of nucleic acid hybridization using polymerization-based amplification. *Anal. Biochemistry* **2009**, *386*, 285-287.

[22] Walker, F.M., Ahmad, K.M., Eisenstein, M., and Soh, H.T. **2014**. "Transformation of Personal Computers and Mobile Phones into Genetic Diagnostic Systems." *Analytical Chemistry*, **86**, 9236-9241.

[23] Engvall, E., and Perlmann, P. **1971**. "Enzyme-linked immunosorbent assay (ELISA) quantitative assay of immunoglobulin G." *Immunochemistry*, **8**, 871-874.

[24] Tuerk, C., and Gold, L. **1990**. "Systematic evolution of ligands by exponential enrichment: RNA ligands to bacteriophage T4 DNA-polymerase." *Science*, **249**, 505-510.

[25] Ellington, A.D., and Szostak, J.W. **1990**. "*In vitro* selection of RNA molecules that bind specific ligands." *Nature*, **346**, 818-822.

[26] Robertson, D.L., and Joyce, G.F. **1990**. "Selection *in vitro* of an RNA enzyme that specifically cleaves single-stranded DNA". *Nature*, **344**, 467-468.

[27] Stone, S.R., and Tapparelli, C. **1994**. "Thrombin Inhibitors and Antithrombotic Agents: The Importance of Rapid Inhibition." *Journal of Enzyme Inhibition*, **9**, 3-15.

[28] Stojanovic, M.N., de Prada, P., and Landry, D.W. **2001**. "Aptamer-Based Folding Fluorescent Sensor for Cocaine." *Journal of the American Chemical Society*, **123**, 4928-4931.

[29] Tombelli, S., Minunni, M., and Mascini, M. **2007**. "Analytical applications of aptamers." *Proceedings of SPIE: International Society of Optical Engineering*, **6565**, 65850W.

[30] Cho, E.J., Lee, J.W., and Ellington, A.D. **2009**. "Applications of Aptamers as Sensors." *Annual Review of Analytical Chemistry*, **2**, 241-264.

[31] Deng, B., Lin, Y., Wang, C., Li, F., Wang, Z., Zhang, H., Li, X.F., and Le, X.C. **2014**. "Aptamer binding assays for proteins: The thrombin example – A review." *Analytica Chimica Acta*, **837**, 1-15.

[32] Griffin, L.C., Toole, J.J., and Leung, L.L.K. **1993**. "The discovery and characterization of a novel nucleotide-based thrombin inhibitor." *Gene*, **137**, 25-31.

[33] Burge, S. Parkingson, G.N., Hazel, P., Todd, A.K., and Neidle, S. **2006**. "Quadruplex DNA: Sequence, topology and structure." *Nucleic Acids Research*, **34**, 5402-5415.

[34] Bochman, M.L., Paeschke, K., and Zakian, V.A. **2012**. "DNA secondary structures: stability and function of G-quadruplex structures." *Nature Reviews Genetics*, **13**, 770-780.

[35] Tasset, D.M., Kubik, M.F., and Steiner, W. **1997**. "Oligonucleotide Inhibitors of Human Thrombin that Bind Distinct Epitopes." *Journal of Molecular Biology*, **272**, 688-698.

[36] Cho, M., Oh, S.S., Nie, J., Stewart, R., Radeke, M.J., Eisentein, M., Coffey, P.J., Thomson, J.A., and Soh, H.T. **2015**. "Array-based Discovery of Aptamer Pairs." *Analytical Chemistry*, **87**, 821-828.

[37] Ahmad, K.M., Xiao, Y., and Soh, H.T. **2012**. "Selection is more intelligent than design: imporving the affinity of a bivalent ligand through directed evolution." *Nucleic Acids Research*, **40**, 11777-11783.

[38] Song, S., Wang, L., Li, J., Fan, C., and Zhao, J. **2008**. "Aptamer-based biosensors." *Trends in Analytical Chemistry*, **27**, 108-117.

[39] Bunka, D.H.J., and Stockley, P.G. **2006**. "Aptamers come of age – at last." *Nature Reviews Microbiology,* **4**, 588-596.

[40] Lauhon, C.T., and Szostak, J.W. **1995**. "RNA aptamers that bind flavin and nicotinamide redox cofactors." *Journal of the American Chemical Society*, **117**, 1246-1257.

[41] Travascio, P., Bennet, A.J., Wang, D.J., and Sen, D. **1999**. "A ribozyme and catalytic DNA with peroxidase activity: active site versus cofactor-binding sites." *Chemical Biology*, **6**, 779-787.

[42] Walsh, R., and DeRosa, M.C. **2009**. "Retention of function in the DNA homolog of the RNA dopamine aptamer." *Biochemical and Biophysical Research Communications*, **388**, 732-735.

[43] Thiel, K.W., and Giangrande, P.H. **2009**. "Therapeutic Applications of DNA and RNA Aptamers." *Oligonucleotides*, **19**, 209-222.

[44] Gold, L., Walker, J.J., Wilcox, S.K., and Williams, S. **2012**. "Advances in human proteomics at high scale with the SOMAscan proteomics platform." *Nature Biotechnology*, **29**, 543-539.

[45] Liu, J., Lee, J.H., and Lu, Y. **2007**. "Quantum Dot Encoding of Aptamer-Linked Nanostructures for One-Pot Simultaneous Detection of Multiple Analytes." *Analytical Chemistry*, **79**, 4120-4125.

[46] Johannsen, B., Noll, B., Leibnitz, P., Reck, G., Noll, S., and Spies, H. **1993**. "Technetium and rhenium complexes of mercapto-containing peptides 1. Tc(V) and Re(V) complexes with mercaptoacetyl diglycine (MAG_2) and X-ray structure of $AsPh_4[TcO(MAG_2)]\bullet C_2H_5OH$." *Inorganica Chimica Acta*, **210**, 209-214.

[47] Da Pieve, C., Perkins, A.C., and Missailidis, S. **2009**. "Anti-MUC1 aptamers: radiolabelling with ^{99m}Tc and biodistribution in MCF-7 tumour-bearing mice." *Nuclear Medicine and Biology*, **36**, 703-710.

[48] Bock, L.C., Griffin, L.C., Latham, J.A., Vermaas, E.H., and Toole, J.J. **1992**. "Selection of single-stranded DNA molecules that bind and inhibit human thrombin." *Nature*, **355**, 564.

[49] Jiang, Y., Fang, X., and Bai, C. **2004**. "Signaling Aptamer/Protein Binding by a Molecular Light Switch Complex." *Analytical Chemistry*, **76**, 5230-5235.

[50] Fang, X., Cao, Z., Beck, T., and Tan, W. **2001**. "Molecular Aptamer for Real-Time Oncoprotein Platelet-Derived Growth Factor Monitoring by Fluorescence Anisotropy." *Analytical Chemistry*, **73**, 5753-5757.

[51] Stojanovic, M.N., de Prada, P., and Landry, D.W. **2000**. "Fluorescent Sensors Based on Aptamer Self-Assembly." *Journal of the American Chemical Society*, **122**, 11547-11548.

[52] Nutiu, R., and Li, Y. **2003**. "Structure-Switching Signaling Aptamers." *Journal of the American Chemical Society,* **125**, 4771-4778.

[53] Nutiu, R., and Li, Y. **2005**. "In Vitro Selection of Structure-Switching Signaling Aptamers." *Angewandte Chemie*, **117**, 1085-1089.

[54] Protein Data Bank. http://www.pdb.org (accessed April 12, 2016).

[55] Nutiu, R., and Li, Y. **2004**. "Structure-Switching Signaling Aptamers: Transducing Molecular Recognition into Fluorescence Signaling." *Chemistry A European Journal,* **10**, 1868-1876.

[56] Chen, J., Fang, Z, Liu, J., and Zeng, L. **2012**. "A simple and rapid biosensor for ochratoxin A based on a structure-switching signaling aptamer." *Food Control*, **25**, 555-560.

[57] Lau, P.S., Lai, C.K., and Li, Y. **2013**. "Quality Control Certification of RNA Aptamer-Based Detection." *ChemBioChem*, **14**, 987-992.

[58] Xia, Y., Gao, P., Qiu, X., Gan, S., Yang, H., and Huang, S. **2012.** "Aptasensor based on triplex switch for SERS detection of cytochrome c." *Analyst*, **137**, 5705-5709.

[59] Cunningham, J.C., Brenes, N.J., and Crooks, R.M. **2014.** "Paper Electrochemical Device for Detection of DNA and Thrombin by Target-Induced Conformational Switching." *Analytical Chemistry*, **86**, 6166-6170.

[60] Sun, L., Frykholm, K., Fornander, L.H., Svedhem, S., Weserlund, F., and Åkerman, B. **2014**. "Sensing Conformational Changes in DNA upon Ligand Binding Using QCM-D. Polyamine Condensation and Rad51 Extension of DNA layers." *Journal of Physical Chemistry B,* **118**, 11895-11904.

[61] Sorgenfrei, S., Chiu, C., Gonzalez Jr., R.L., Yu, Y-J., Kim, P., Nuckolls, C., and Shepard, K.L. **2011.** "Label-free single-molecule detection of DNA-hybridization kinetics with a carbon nanotube field-effect transistor." *Nature Nanotechnology*, **6**, 126-132.

[62] Tavares, A.J., Noor, M.O., Uddayasankar, U., Krull, U.J., and Vannoy, C.H. **2014.** "Solid-Phase Supports for the in situ Assembly of Quantum Dot-FRET Hybridization Assays in Channel Microfluidics." *Methods in Molecular Biology*, **1199**, 241-255.

[63] Liu, X., Freeman, R., Golub, E., and Willner, I. **2011.** "Chemiluminescence and Chemiluminescence Resonance Energy Transfer (CRET) Aptamer Sensors Using Catalytic Hemin/G-Quadruplexes." *ACS Nano*, **5**, 7648-7655.

[64] Zhao, T., Liu, R., Ding, X., Zhao, J., Yu, H., Wang, L., Xu, Q., Wang, X., Lou, X., He, M., and Xiao, Y. **2015**. "Nanoprobe-Enhanced, Split Aptamer-Based Electrochemical Sandwich Assay for Ultrasensitive Detection of Small Molecules." *Analytical Chemistry,* **87**, 7712-7719.

[65] Alsager, O.A., Kumar, S., Zhu, B., Travas-Sejdic, J., McNatty, K.P., and Hodgkiss, J.M. **2015**. "Ultrasensitive Colorimetric Detection of 17β-Estradiol: The Effect of Shortening DNA Aptamer Sequences." *Analytical Chemistry*, **87**, 4201 – 4209.

[66] Bonham, A.J., Hsieh, K., Ferguson, B.S., Vallée-Bélisle, A., Ricci, F., Soh, H.T., and Plaxco, K.W. **2012.** "Quantification of Transcription Factor Binding in Cell Extracts Using an Electrochemical, Structure-Switching Biosensor." *Journal of the American Chemical Society,* **134**, 3346-3348.

[67] Zhuang, J., He, Y., Chen, G., and Tang, D. **2014**. "Binding-induced internal-displacement of inverted aptamer beacon: Toward a novel electrochemical detection platform." *Electrochemistry Communications,* **47**, 25-28.

[68] Vallée-Bélisle, A., Bonham, A.J., Reich, N.O., Ricci, F., and Plaxco, K.W. **2011**. "Transcription Factor Beacons for the Quantitative Detection of DNA Binding Activity." *Journal of the American Chemical Society*, **133**, 13836-13839.

[69] Tyagi, S., and Kramer, F.R. **1995**. "Molecular Beacons: Probes that Fluoresce upon Hybridization." *Nature Biotechnology,* **14**, 303-308.

[70] Guo, J., Ju, J., and Turro, N.J. **2012**. "Fluorescent hybridization probes for nucleic acid detection." *Analytical and Bioanalytical Chemistry,* **402**, 3115-3125.

[71] Watzinger, F., Ebner, K., and Lion, T. **2006.** "Detection and monitoring of virus infections by real-time PCR." *Molecular Aspects of Medicine*, **27**, 254-298.

[72] Fang, X., Mi, Y., Li, J.J., Beck, T., Schuster, S., and Tan, W. **2002**. "Molecular beacons: Fluorogenic probes for living cell study." *Cell Biochemistry and Biophysics,* **37**, 71-81.

[73] Hamaguchi, N., Ellington, A., and Stanton, M. **2001**. "Aptamer Beacons for the direct detection of proteins." *Analytical Biochemistry,* **294**, 126-131.

[74] Liu, J., Cao, Z., and Lu, Y. **2009**. "Functional Nucleic Acid Sensors." *Chemical Reviews,* **109**, 1948-1998.

[75] Nutiu, R., and Li, Y. **2003**. "Structure-Switching Signaling Aptamers." *Journal of the American Chemical Society,* **125**, 4771-4778.

[76] Zheng, D., Zou, R., and Lou, X. **2012**. "Label-Free Fluorescent Detection of Ions, Proteins, and Small Molecules Using Structure-Switching Aptamers, SYBR Gold, and Exonuclease I." *Analytical Chemistry*, **84**, 3554-3560.

[77] Tanaka, K., Yamada, Y., and Shinoya, M. **2002**. "Formation of Silver(I)-Mediated DNA Duplex and Triplex through an Alternative Base Pair of Pyridine Nucleobases." *Journal of the American Chemistry Society,* **124**, 8802-8803.

[78] Porchetta, A., Vallée-Bélisle, A., Plaxco, K.W., and Ricci, R. **2013**. "Allosterically Tunable, DNA-Based Switches Triggered by Heavy Metals." *Journal of the American Chemical Society,* **135**, 13238-13241.

[79] Clever, G.H., Kaul, C., and Carell, T. **2007.** "DNA-Metal Base Pairs." *Angewandte Chemie International Edition,* **46**, 6226-6236.

[80] Bury, N.R., McGeer, J.C., and Wood, C.M. **1999**. "Effects of altering freshwater chemistry on physiological responses of rainbow trout to silver exposure." *Environmental Toxicology and Chemistry,* **18**, 49-55.

[81] Bianchini, A., Grosell, M., Gregory, S.M., and Wood, C.M. **2002**. "Acute Silver Toxicity in Aquatic Animals Is a Function of Sodium Uptake Rate." *Environmental Science and Technology,* **36**, 1763-1766.

[82] Cheung, Y.W., Kwok, J., Law, A.W.L., Watt, R.M., Kotaka, M., and Tanner, J.A. **2013**. "Structural basis for discriminatory recognition of *Plasmodium* lactate dehydrogenase by a DNA aptamer." *Proceedings of the National Academy of Sciences of the United States of America,* **110**, 15967-15972.

[83] Tan, X., Chen, W., Lu, S., Zhu, Z., Chen, T., Zhu, G., You, M., and Tan, W. **2012**. "Molecular Beacon Aptamers for Direct and Universal Quantitation of Recombinant Proteins from Cell Lysates." *Analytical Chemistry*, **84**, 8272-8276.

[84] Doyle, M.B., Murphy, S. A. **2005**. "Aptamers and methods for their in vitro selection and uses thereof." *US Patent Application Publication*, US20050142582 A1, June 30, 2005.

[85] Li, L., Li, B., Qi, Y., and Jin, Y. **2009**. "Label-free aptamer-based colorimetric detection of mercury ions in aqeous media using unmodified gold nanoparticles as colorimetric probe." *Analytical and bioanalytical Chemistry*, **393**, 2051-2057.

[86] Xia, F., Zuo, X., Yang, R., Xiao, Y., Kang, D., Vallée-Bélisle, A., Gong, X., Yuen, J.D., Hsu, B.B.Y., Heeger, A.J., and Plaxco, K.W. **2010**. "Colorimetric detection of DNA, small molecules, proteins, and ions using unmodified gold nanoparticles and conjugated polyelectrolytes." *Proceedings of the National Academy of Sciences of the United States of America*, **107**, 10837-1041.

[87] Porchetta, A., Vallée-Bélisle, A., Plaxco, K.W., and Ricci, F. **2013**. "Allosterically tunable, DNA-based switches triggered by heavy metals." *Journal of the American Chemical Society*, **135**, 13238-13241.